JOURNAL OF GEOPHYSICAL RESEARCH, VOL. 97, NO. D13, PAGES 14,581–14,599, SEPTEMBER 20, 1992

Biomass Burning Airborne and Spaceborne Experiment in the Amazonas (BASE-A)

Y. J. KAUFMAN,[1] A. SETZER,[2] D. WARD,[3] D. TANRE,[4,5] B. N. HOLBEN,[4] P. MENZEL,[6] M. C. PEREIRA,[2] AND R. RASMUSSEN[7]

In the Biomass Burning Airborne and Spaceborne Experiment in the Amazonas (BASE-A), conducted in September 1989, trace gas and particulate matter emissions were measured from biomass burning due to deforestation and grassland fires in South America. This information is required for a better understanding of the environmental impacts of biomass burning in the tropics and to improve algorithms for remote sensing of biomass burning from satellite platforms. The field experiment utilized the twin-engine Embraer Bandeirante EMB-101 instrumented aircraft of the Brazilian Institute for Space Research (INPE). Concentrations of ozone, CO_2, CO, CH_4, and particulate matter were measured from the aircraft. Fires were observed from satellite imagery, and the smoke optical thickness, particle size, and profiles of the extinction coefficient were measured using sunphotometers in the aircraft and from the ground. Four smoke plumes were sampled, three vertical profiles were measured, and extensive ground measurements were conducted of smoke optical characteristics for different smoke types. The collected data were analyzed for determining the emission ratios and combustion efficiency (the efficiency of a fire to convert the total burned carbon to carbon dioxide) and were compared with the results from fires in North America. Combustion efficiency was found to be higher in the tropics (97% for the cerrado and 90% for the deforestation fires) with emission factors similar to those of North American fires, for a given combustion efficiency. A strong relation was found between the spatial distribution of fires (up to 9000 per day in one state) and ozone concentration (up to 80 ppbv) and between biomass burning and concentrations of trace gases, particulate matter, and ozone. These relations strongly suggest a correlation between biomass burning in the tropics and ozone formation. An optical model of the smoke aerosol was derived and applied to radiance measurements. The smoke single scattering albedo was computed from the graphitic carbon concentration (assuming external mode mixture) as 0.90 ± 0.01. The particles effective radii were 0.1 to 0.2 μm, except for 1-day aged smoke with values up to 0.4 μm. Radiance measurements indicate that the width of the particle size distribution may be smaller in the tropics than for North American fires. The measured optical properties of smoke and the high correlation between emitted trace gases and particles form a basis for remote sensing of radiatively important trace gases and particulate matter from biomass burning using AVHRR imagery.

1. INTRODUCTION

Biomass burning is a major source of trace gas emission into the troposphere (e.g., CO_2, CH_4, CO, NO_x, CH_3Cl, etc. [*Seiler and Crutzen*, 1980; *Crutzen et al.*, 1985; *Ward*, 1986]). The increased rate of biomass burning in the last decade [*Tucker et al.*, 1984; *Malingreau et al.*, 1988] is mainly due to the expansion of deforestation in the Amazon basin [*Setzer et al.*, 1988; *Setzer and Pereira*, 1990; *Kaufman et al.*, 1990*a*] and from an increasing rate of burning of cultivated areas in the African savanna from once every 3 to 5 years to once every 1 to 2 years [*Seiler and Crutzen*, 1980; *Hao et al.*, 1990]. Some of these emission gases (CO_2, CH_4, and CH_3Cl) participate in the greenhouse effect that heats the atmosphere [*Ramanathan et al.*, 1985]. Other gases (e.g., NO_x and CH_4) act as reactive gases that affect atmospheric chemistry [*Crutzen*, 1988]. The emitted gases (e.g., CH_4, CO, and NO_x) are involved in complex chemical reactions in the troposphere, causing elevated levels of ozone [*Fishman et al.*, 1979; *Andreae et al.*, 1988, 1992; *Setzer and Pereira*, 1990; *Crutzen*, 1988] and acid precipitation [*Crutzen and Andreae*, 1990].

Biomass burning is also a major source of organic hygroscopic particles [*Greenberg et al.*, 1984; *Crutzen et al.*, 1985; *Ward*, 1986; *Andreae et al.*, 1988; *Ward et al.*, 1990]. These smoke particles were observed to affect cloud microphysics [*Twomey and Warner*, 1967; *Warner and Twomey*, 1967; *Hobbs and Radke*, 1969], by increasing the available cloud condensation nuclei [*Squires and Twomey*, 1960; *Radke*, 1989], and as a result, to generate brighter clouds that reflect solar radiation to space [*Twomey et al.*, 1984; *Coakley et al.*, 1987; *Radke*, 1989; *Wigley*, 1989; *Kaufman et al.*, 1990*b*; Y. J. Kaufman and M.-D. Chou, Model simulations of the competing climatic effects of SO_2 and CO_2, submitted to *Journal of Climate*, 1991]. These particles can also cool the climate by directly reflecting solar radiation to space [*Coakley et al.*, 1983]. For stratiform clouds it was shown that the polluted clouds, having smaller cloud droplets, result in less precipitation [*Albrecht*, 1989; *Radke et al.*, 1990]. Biomass burning emits also graphitic carbon, a black material, that can increase absorption of solar radiation by the atmosphere [*Ackerman and Toon*, 1981] and by clouds [*Twomey*, 1977; *Twomey et al.*, 1984]. This effect can cause heating of the atmosphere and therefore may counteract the radiative effect of the organic particles. The graphitic carbon may be

[1]NASA Goddard Space Flight Center, Laboratory for Atmospheres, Greenbelt, Maryland.
[2]Instituto de Pesquisas Espaciais, San Jose dos Campos, São Paulo, Brazil.
[3]USDA Forest Service Fire Chem, Missoula, Montana.
[4]NASA Goddard Space Flight Center, Greenbelt, Maryland.
[5]On leave from Laboratoire d'Optique Atmosphérique, Université de Sciences et Techniques de Lille, Villeneuve d'Ascq, France.
[6]NOAA/NESDIS Satellite Applied Laboratory, Madison, Wisconsin.
[7]Oregon Graduate Institute, Beaverton.

Paper number 92JD00275.
0148-0227/92/92JD-00275$05.00

emitted in the form of separate particles, or serve as the condensation nuclei for the organic, hygroscopic particles.

The estimation of the magnitude of biomass burning and its atmospheric effects is difficult due to the fragmented distribution of the areas burned and the diversity of type of fires and burned vegetation. It is difficult to monitor the frequency of burns and the duration of each fire [*Kaufman et al.*, 1990*a*]. Present estimates of emissions from biomass burning are based on economic statistics [*Crutzen et al.*, 1979; *Woodwell and Houghton*, 1983; *Hao et al.*, 1990]. Estimates of biomass burning emissions can be improved by remote sensing techniques [*Tucker et al.*, 1984; *Malingreau and Tucker*, 1988; *Setzer et al.*, 1988; *Setzer and Pereira*, 1990, 1991; *Kaufman et al.*, 1990*a*] calibrated through the collection of ground truth information (e.g., measurements in North America [*Ward and Hardy*, 1984] and in Brazil [*Ward et al.*, this issue]).

The Biomass Burning Airborne and Spaceborne Experiment-Amazonas (BASE-A), reported in this paper, was designed to provide such information. Previous field experiments in the Amazon basin reported measurements of the relations among biomass burning, the emission of trace gases, and the production of ozone. The present field experiment updates this information and measures simultaneously two additional parameters that are important for remote sensing of biomass burning: smoke particles and the distribution of fires. The principal objective for BASE-A research includes the development of a relation between the emitted trace gases and smoke particles and to measure the optical characteristics of the smoke particles and their effect on upward radiation as detected by satellites. The simultaneous measurement of the trace gases (e.g., CO, CH_4), ozone, smoke particles, and the distribution of fires is used to clarify the link between biomass burning and the elevated levels of ozone. In section 2 the present status of remote sensing of biomass burning from satellite platforms is reviewed and a summary is given identifying those parameters still needing quantification from field experiments to improve the overall accuracy. The measurement techniques and instrumentation used in BASE-A are described in section 3. The BASE-A experiment is described in section 4 and results are reported in section 5. In section 6 the summary of the results is given and implications to satellite remote sensing are discussed. Section 7 concludes this paper.

2. REMOTE SENSING OF BIOMASS BURNING AND EMISSION PRODUCTS: RATIONALE FOR BASE-A

In this section we shall review the present satellite remote sensing capabilities to detect (directly and indirectly) emissions from biomass burning and shall discuss the parameters that have to be measured in field experiments in order to develop these remote sensing techniques. These requirements form the rationale for the BASE-A experiment reported in this paper.

Fires. Using the advanced very high resolution radiometer (AVHRR), 1-km resolution, 3.75-μm and 11-μm channels, it is possible to sense the presence of fires as small as 10 m × 10 m [*Matson and Dozier*, 1981; *Setzer et al.*, 1988; *Setzer and Pereira*, 1991; *Kaufman et al.*, 1990*a*; *Lee and Tag*, 1990]. AVHRR sensors on board NOAA 10 and 11 provide daily morning, afternoon, early evening, and night images of the globe and can be used to monitor the frequency of occurrence and spatial distribution of fires. Because of the low-saturation level of the 3.75-μm channel (318° to 320°K) some land areas are hot enough to saturate the afternoon images.

Detection of fires in the Brazilian Amazon, using the AVHRR, was developed by *Pereira* [1988] and is in operational use at the Brazilian Institute for Space Research (Instituto de Pesquisas Espaciais (INPE)) [*Setzer and Pereira*, 1990, 1991]. The direct relation between fires observed from the AVHRR imagery and smoke layers hundreds of kilometers downwind in Amazonia was reported [*Andreae et al.*, 1988; *Kirchhoff et al.*, 1989*a*, *b*]. Although not all the fires can be detected, and the fire count does not distinguish between large and small fires, a direct relation between the fires and the deforestation area was found [*Setzer et al.*, 1990] as well as between fire count and the mass of the emitted smoke particles [*Kaufman et al.*, 1990*a*]. Therefore fire count, together with remote sensing of deforestation or smoke particles, can be used to estimate emissions of particles and trace gases from biomass burning. Fires can also be detected from the Geostationary Operational Environmental Satellite (GOES) visible infrared spin scan radiometer (VISSR) atmospheric sounder (VAS) 7-km resolution imagery [*Menzel et al.*, 1990; *Prins and Menzel*, 1990]. Because of the lower spatial resolution, only large fires can be detected (the active fire area for temperature $\geq$450°K should be $\geq$0.03 km^2), but the diurnal cycle of the fires can be obtained from the twice hourly imagery.

One of the objectives of the BASE-A experiment is to determine the relationship between fires observed from the AVHRR, GOES-VAS, and fires on the ground and to establish the relation between the spatial distribution of fires and the rate of emission of trace gases and smoke particles and the production of ozone.

Deforestation. Using the same AVHRR 1-km data at 3.75 μm, *Tucker et al.* [1984] and *Malingreau and Tucker* [1988] monitored deforestation of Rondonia, Brazil. This work has expanded using higher-resolution TM data for the entire Amazon basin (C. J. Tucker, personal communication, 1991).

A variation of the deforestation approach is burn scar monitoring usually requiring high-resolution data (80 m or better) and more timely data. *Setzer et al.* [1988] and *Setzer and Pereira* [1990] used estimates of the area of burn scars from the 80-m resolution Landsat multispectral spectrometer (MSS) sensor to "calibrate" deforestation associated with fires observed from the AVHRR. Using published data on biomass density and emission ratios, they were able to estimate the total emission of trace gases from deforestation of the Brazilian Amazon forest. The BASE-A experiment was designed to provide in situ measurements of the emission ratios and to compare these ratios with the literature values.

Smoke particles. From the AVHRR visible and near-IR images taken over vegetated terrain, it is possible to derive the smoke optical thickness (proportional to the particle mass loading) and its single scattering albedo (a measure of the particle absorption). This method was applied to images of North America [*Kaufman*, 1987; *Kaufman et al.*, 1990*b*; *Ferrare et al.*, 1990] and to images of the Amazon basin [*Kaufman et al.*, 1990*a*]. Smoke particles are one of the emission products and are highly correlated with the emitted

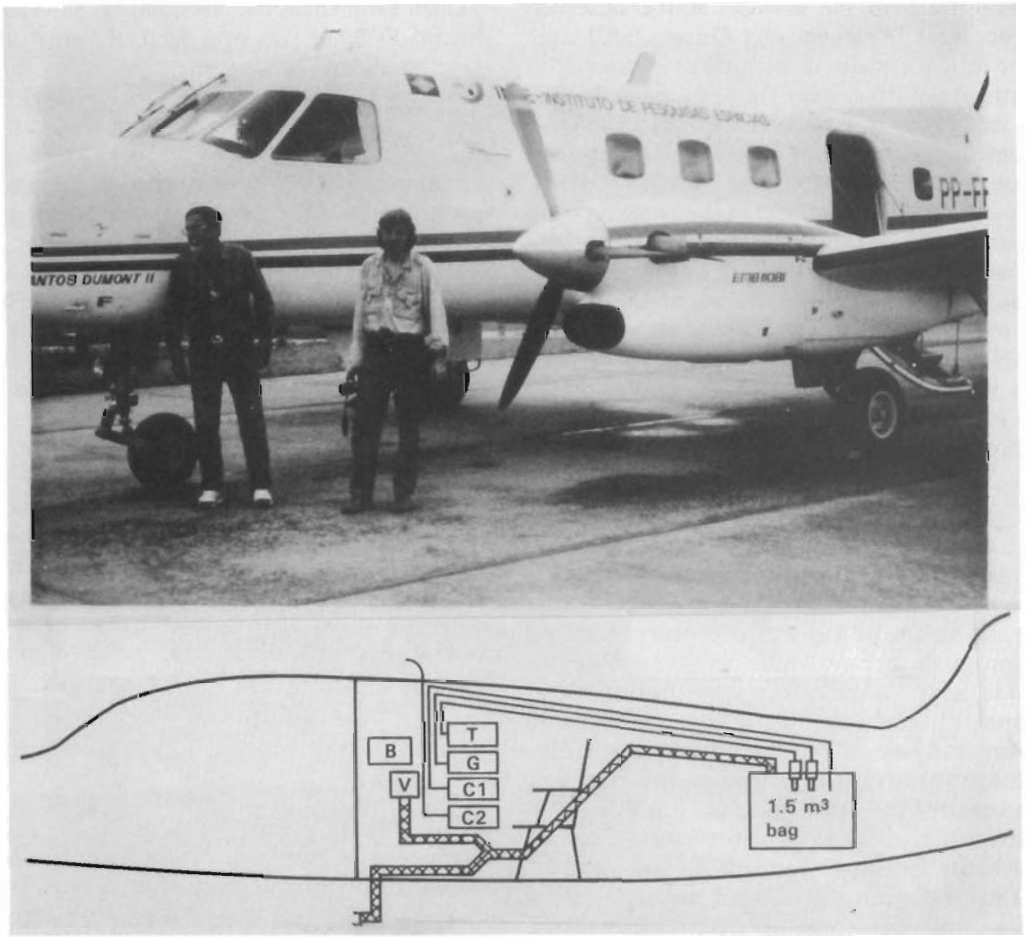

Fig. 1. Schematic of sampling apparatus used on board the INPE aircraft for sampling emissions from biomass fires in Brazil. B, Buck calibrator; T, Teflon filter 2 L/min pump; G, glass filter 2 L/min pump; C1 and C2, pump to fill canisters from bag and from aircraft exterior, respectively.

ure 1) on the INPE aircraft. A stainless steel tube was used for the trace gas sample collection, and a second independent system was used for sampling the high-concentration plumes over short spatial regions of the plumes.

In-plume sampling was done using a system consisting of a plastic polyvinyl chloride (PVC) sample probe (38 mm in diameter) that extended from outside the aircraft to a large (1.5-m^3) polyethylene sample bag in the aircraft. The probe was designed to sample from under the fuselage well in front of any possible influence from the engine exhaust or wings of the aircraft. The bag required 10 s to fill and integrated the sample over a 500-m path length. After each sample, the large bag was flushed with ambient air and evacuated before repeating the sampling protocol. Similar systems have been used for airborne studies in the United States [*Einfeld et al.*, 1991; *Radke et al.*, 1990]. Although losses due to electrically charged particles are possible with the 1.5-m^3 sample bag, the results of others using the same type of sample bag and from independent measurements of particles directly onto filters would suggest these losses to be minimal [*Ward and Hardy*, 1991; *Einfeld et al.*, 1991; *Radke et al.*, 1991].

Subsampling of particles less than 2.5 μm in diameter (PM2.5) was accomplished onto pairs of 37-mm filters (one Teflon and one glass fiber filter) from the large bag through a cyclone. These filters were used for measurements of mass loading of particles of PM2.5 and the content of the particles for inorganic and organic fractions. The aerosol samples were sampled at a rate of 2 L/min over 15- to 20-min periods. The PM2.5 concentration was calculated as the ratio of the total mass collected on the filters and the total flow through the filters. A soap bubble calibrator was used at each altitude to sample the volume flow of the pumps and then corrected for temperature and pressure. CO_2, CO, and CH_4 concentrations were determined from canister samples collected from the large bag. These canisters were pumped to 2 atmospheres pressure and returned to the United States for analysis using gas chromatography procedures.

Ambient gas samples were collected in canisters through a stainless steel tube extending to the outside of the aircraft. These canisters were also returned to the United States for analysis.

3.6. *Optical Measurements of Smoke Particles*

Measurement of the optical properties of smoke emitted from biomass burning in Brazil required a multitemporal and multielevational approach to characterize background conditions of the smoke particles, fresh and aged smoke from the flaming phase, fresh smoke from the smoldering phase, and a mixture of all (see Plate 1). Sunphotometers were used at ground level and from the INPE aircraft to measure the spectral solar irradiance that is directly transmitted from the

Plate 1. Smoke and fire due to deforestation in Brazil showing typical atmospheric conditions during measurements for BASE-A: (top) condition of measurements of smoke optical thickness and particle size by observations of the Sun through the smoke and (bottom) smoke originating from fires on the ground, rising through the atmosphere to the condensation level, forming clouds, and diffusing into a smoke layer.

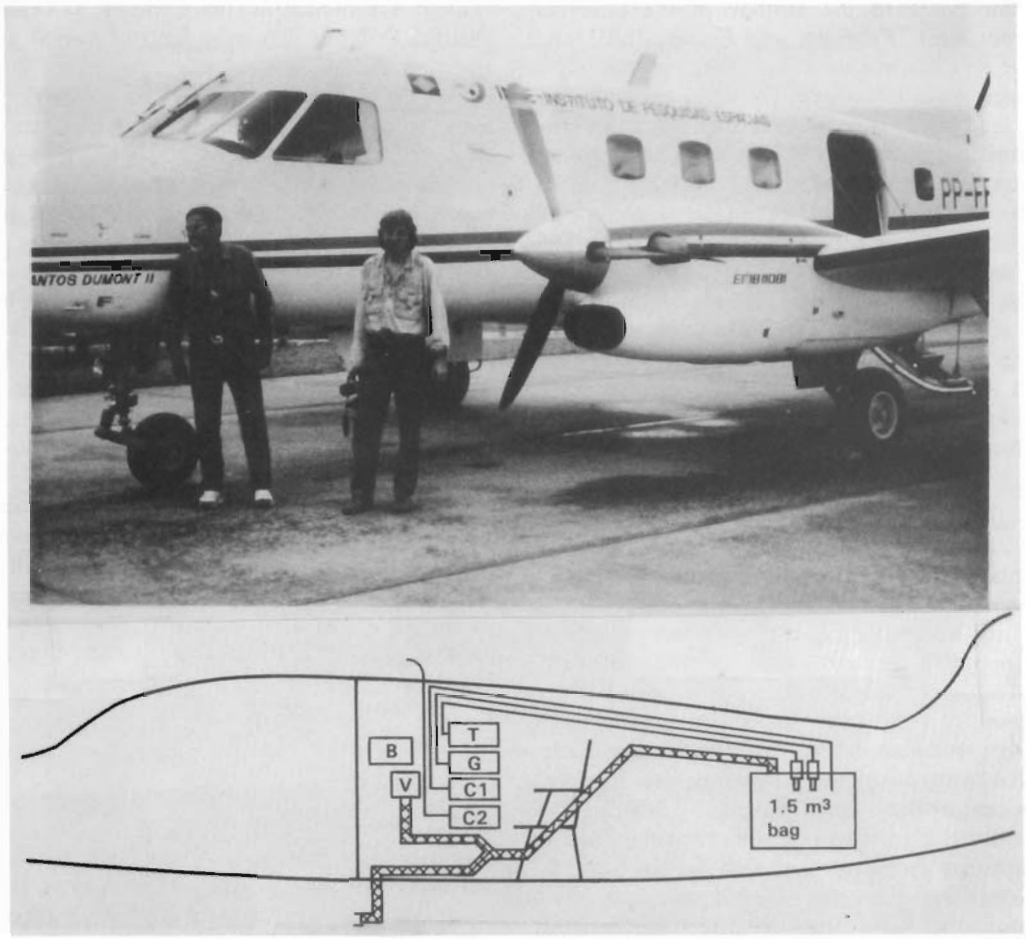

Fig. 1. Schematic of sampling apparatus used on board the INPE aircraft for sampling emissions from biomass fires in Brazil. B, Buck calibrator; T, Teflon filter 2 L/min pump; G, glass filter 2 L/min pump; C1 and C2, pump to fill canisters from bag and from aircraft exterior, respectively.

ure 1) on the INPE aircraft. A stainless steel tube was used for the trace gas sample collection, and a second independent system was used for sampling the high-concentration plumes over short spatial regions of the plumes.

In-plume sampling was done using a system consisting of a plastic polyvinyl chloride (PVC) sample probe (38 mm in diameter) that extended from outside the aircraft to a large (1.5-m^3) polyethylene sample bag in the aircraft. The probe was designed to sample from under the fuselage well in front of any possible influence from the engine exhaust or wings of the aircraft. The bag required 10 s to fill and integrated the sample over a 500-m path length. After each sample, the large bag was flushed with ambient air and evacuated before repeating the sampling protocol. Similar systems have been used for airborne studies in the United States [*Einfeld et al.*, 1991; *Radke et al.*, 1990]. Although losses due to electrically charged particles are possible with the 1.5-m^3 sample bag, the results of others using the same type of sample bag and from independent measurements of particles directly onto filters would suggest these losses to be minimal [*Ward and Hardy*, 1991; *Einfeld et al.*, 1991; *Radke et al.*, 1991].

Subsampling of particles less than 2.5 μm in diameter (PM2.5) was accomplished onto pairs of 37-mm filters (one Teflon and one glass fiber filter) from the large bag through a cyclone. These filters were used for measurements of mass loading of particles of PM2.5 and the content of the particles for inorganic and organic fractions. The aerosol samples were sampled at a rate of 2 L/min over 15- to 20-min periods. The PM2.5 concentration was calculated as the ratio of the total mass collected on the filters and the total flow through the filters. A soap bubble calibrator was used at each altitude to sample the volume flow of the pumps and then corrected for temperature and pressure. CO_2, CO, and CH_4 concentrations were determined from canister samples collected from the large bag. These canisters were pumped to 2 atmospheres pressure and returned to the United States for analysis using gas chromatography procedures.

Ambient gas samples were collected in canisters through a stainless steel tube extending to the outside of the aircraft. These canisters were also returned to the United States for analysis.

3.6. *Optical Measurements of Smoke Particles*

Measurement of the optical properties of smoke emitted from biomass burning in Brazil required a multitemporal and multielevational approach to characterize background conditions of the smoke particles, fresh and aged smoke from the flaming phase, fresh smoke from the smoldering phase, and a mixture of all (see Plate 1). Sunphotometers were used at ground level and from the INPE aircraft to measure the spectral solar irradiance that is directly transmitted from the

top of the atmosphere to the altitude of the observer. Calibration procedures [*Kaufman and Fraser*, 1983] were used to find the sunphotometer reading that corresponds to the extraterrestrial solar irradiance. The absolute calibration of the aircraft instrument was obtained by cross calibration with a spectrometer calibrated by viewing the Sun from a tethered balloon at an altitude of 30 km [*Tanre et al.*, 1988]. The ratio of the solar irradiance measured from the ground to the extraterrestrial solar irradiance is the transmission (T) through the atmosphere.

The airborne sunphotometer was operated through an open window of the INPE aircraft. Profiles were made at heights (h) from 300 to 4000 m from the surface in approximately 600-m intervals. Profiles of the transmission (T) were inverted into profiles of the extinction coefficient (κ) using the relation

$$\kappa = -\frac{d \ln T}{dh} \quad (1)$$

Measurements of the extinction coefficient were carried by a sunphotometer at three spectral wavelengths: 0.45, 0.65, and 0.85 μm, and water vapor profiles were measured by the same sunphotometer from a ratio of broad and narrow bands centered in the water vapor absorption region 0.935 to 0.950 μm [*Tanre et al.*, 1988]. Measurements from the ground of the optical characteristics of the smoke particles were conducted with a similar sunphotometer but with spectral bands centered at 0.500, 0.875, and 0.945 μm. The spectral characteristics of the extinction coefficient and of the optical thickness measured from the ground were inverted into the particle mean size (see section 5.4.1).

The sunphotometers were cross calibrated immediately before, during, and after the BASE-A experiment. It was found that the aerosol optical thickness can be measured to a precision of ± 0.02 and an accuracy of ± 0.05. The precision of calibration between the spectral bands is estimated to be ± 0.02. These relatively large uncertainties resulted from instabilities detected in one or more of the sunphotometers. The extinction coefficient is not sensitive to the uncertainty in the absolute calibration but is sensitive to spatial nonhomogeneities in the atmosphere. Water vapor retrievals were compared to measured radiosondes at Dulles Airport near Washington, D. C., and found to agree within ± 0.4 cm for total column water vapor, for a range of 1 to 5 cm of water. Water vapor profiles are also affected by the time difference between measurements taken from the different atmospheric layers. Because of spatial nonhomogeneity of the atmosphere and changes with time some random errors in the measured water vapor profile can be introduced. It is expected that the error in the water vapor profiles is ± 0.5 cm/km.

4. THE FIELD EXPERIMENT

The INPE aircraft was flown from San Jose dos Campos to Brasilia and northward to Alta Floresta. Figure 2 shows the airplane trajectory superimposed on a 4-day composite of AVHRR fire count in the region, taken between September 1 and 7, 1989. Figure 3*a* shows the flight levels during BASE-A. The flight levels are a combination of the attempt to monitor the contaminations of the lower troposphere as well as flight restrictions. Flight information is summarized in Table 1.

Flight 1 from San Jose dos Campos, São Paulo, to Brasilia, Distrito Federal, was over land of varied use but mainly agricultural with sugar cane plantations that are burned before harvesting [*Kirchhoff et al.*, 1989*b*]. Flight 2, from Brasilia to Porto Nacional, Tocantins, was over savanna type vegetation ("cerrado") where open pasture is the predominant feature and where fire is regularly used to renew the grasses. Flight 3 began with the transition from cerrado to forest and ended in Alta Floresta, Mato Grosso, an area of fast forest conversion to large ranches. Flights 4–6 were flown in the vicinity of Alta Floresta. Flight 7 covered forested areas where some deforestation is taking place, until Santarem, Para. Flight 8 to Manaus, Amazonas, was over relatively untouched forest. Flight 9 was flown to Porto Velho, Rondonia, where an increase in deforestation and fires toward Rondonia was observed. Flight 10 was over a region where extensive deforestation and burning takes place, in the vicinity of the BR-364 road, and over cerrado areas close to Cuiaba, Mato Grosso, also dominated by the use of fire. Flight 11 to Uberlandia, Mato Grosso, covered areas of intense agriculture, mainly soybean plantations, where fire was being used to burn grasses and weeds before plowing. Flight 12, the last one, covered an area similar to flight 1.

5. RESULTS

5.1. *Fire Detection*

Detection of fires from the AVHRR data is based on the work originally presented by *Matson et al.* [1984]. AVHRR images in band 3 (3.55–3.95 μm) were recorded daily by INPE at Cachoeira Paulista, São Paulo, and screened for "hot" pixels with nominal radiometric brightness temperature between 316° and 320°K, the former being the saturation limit of the sensor. As shown by *Pereira* [1988] and verified by field work, this range indicates major fires occurring at the time the image was produced by the NOAA satellite, around 1400 to 1600 LT (Table 1).

The AVHRR cannot provide the diurnal variability of the biomass burning process. Therefore the 16-km resolution GOES-VAS imagery is used for this purpose. The analysis of the GOES-VAS data is based on the visible and IR image interpretation. A fire was detected if there was an increase in the apparent brightness temperature of at least 4°K in the 3.9-μm channel and 1°K in the 11-μm channel and if the hot pixel was accompanied by a smoke plume observed in the visible channel of GOES-VISSR [*Menzel et al.*, 1990]. A separation between smoke plumes and clouds was based on a time series of the half hourly visible images. While clouds moved as a function of time, the source of the smoke did not move. Fires were detected over the period from 1349 UTC on September 4, 1989, until 0149 UTC on September 5, 1989. The area of the study covered 4° to 10°S and 48° to 60°W, including the location of Alta Floresta. The results are summarized in Table 2, showing the diurnal variability of the fire detection. The maximum number of fires was detected at 1649 UTC. No fires were detected at 0149 UTC. This strong diurnal variability was typical throughout the period of the study [*Menzel et al.*, 1990]. The apparent fire temperature and the subpixel area being burned were also computed [*Menzel et al.*, 1990] by using the 3.9-μm and the 11-μm channels and were given in Table 2.

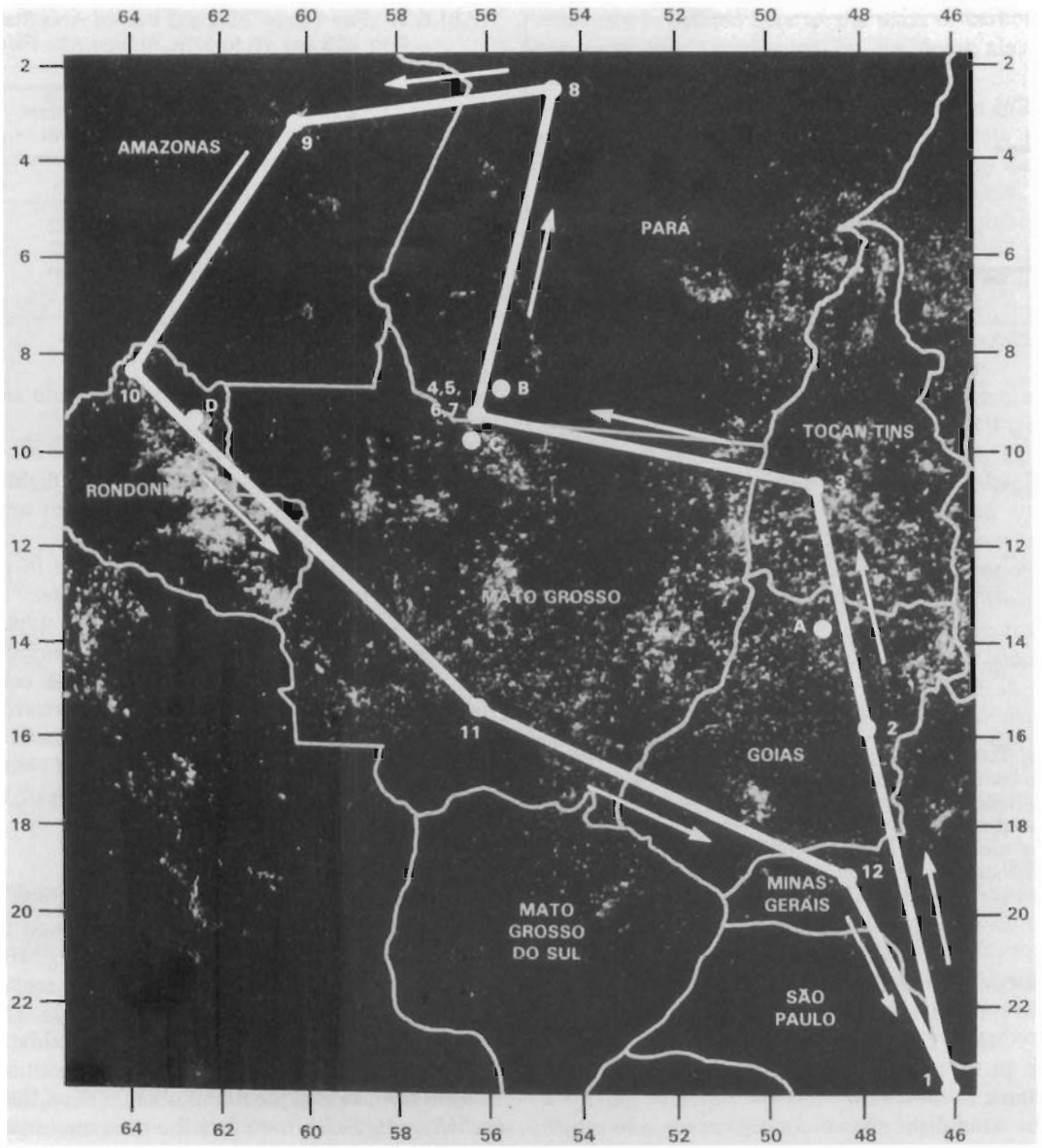

Fig. 2. Approximate trajectory of the flights during BASE-A, superimposed on a 4-day composite of fires in the Amazon basin (taken between September 1 and 7, 1989). The location of plume samples is indicated by letters: A, September 2, 1989, in the cerrado area; B, C, and D, September 3, 4, and 7, respectively, in the forest area.

5.2. *Relation Between Ozone Measurements and Fires*

Figure 3*b* shows ozone concentrations in parts per billion by volume (ppbv) for the flight segments shown in Figures 2 and 3*a* and represents data after flight altitude and ozone readings were stable. Figure 4 shows a comparison between vertical profiles of ozone and profiles of trace gas and extinction coefficient discussed later in section 5.3.3. Ozone concentrations were higher in cerrado and deforestation areas, where biomass burning takes place, than on the Amazonas and North Para areas where fires are rare (Table 1). In the following the ozone concentration and fire count associated with each flight are described:

Flight 1. During this morning flight no fires were observed. Ozone concentration was about 40 ppbv up from 25 ppbv that is considered background (see flight 8). The elevated ozone was possibly caused by diverse agricultural fires in the region and by downwind combustion products brought by prevailing W and NW winds from fires in Goias, Mato Grosso do Sul, and Mato Grosso in the previous day (Table 1).

Flight 2. Ozone ranged 50 to 65 ppbv between Brasilia and Porto Nacional, due to fires in Goias, and would probably have been higher for a flight in the afternoon when ozone-producing photochemical reactions are more efficient.

Flight 3. Ozone was also in the 50 to 60 ppbv during the flight to northern Mato Grosso in the afternoon, affected by concentrated fires in the Tocantins state.

Flight 7. The range of ozone in this flight would have been the same if it had not crossed the plumes from fires in South Para carried by the easterly winds, which caused an increase to about 65 ppbv.

Flight 8. Ozone concentration was the smallest in t' flight, in the 25 ppbv range. This flight was far from f Even the 326 fires detected in the Amazon region

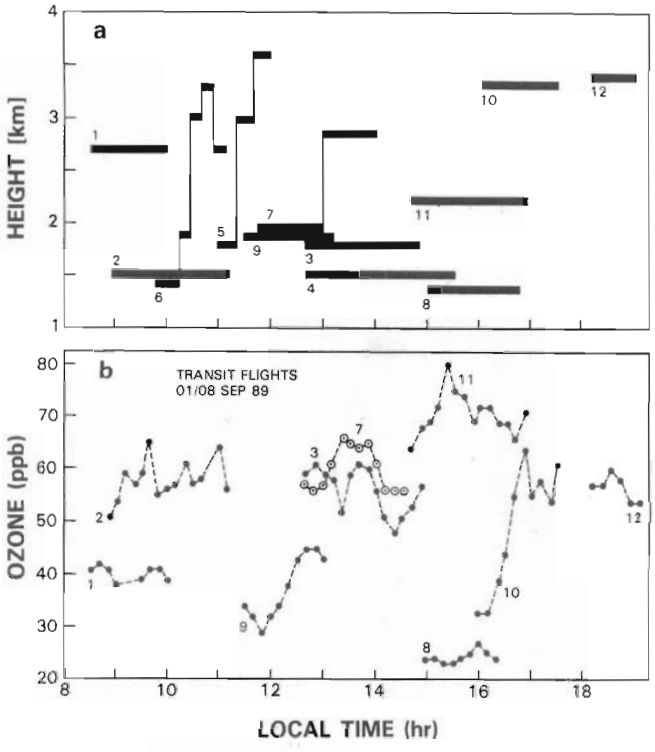

Fig. 3. (*a*) Time and elevation (kilometers) of flights shown in Figure 2. The numbers correspond to flight number in Table 1. (*b*) Ozone concentration (ppbv) for flights indicated in Figures 2 and 3*a*: flight 1, sugar cane fire; flight 2, cerrado fires; flight 3, flight from cerrado to the forest area; flight 7, deforestation fires; flight 8, no fires; flight 9, flight from the Amazonia with no fires to Rondonia where fires are present; flights 10 and 11, fires present.

mostly in parts of Rondonia and Acre that were included in the fire count but did not affect the ozone concentrations.

Flight 9. Ozone concentration increased from 30 to 50 ppbv as the plane approached the Rondonia state where biomass burning is common.

Flight 10. This flight shows a steep increase in ozone, from 35 to 60 ppbv, as the plane moved into areas of more intense biomass burning.

Flight 11. The highest concentrations of ozone, in the 60 to 80 ppbv range, were measured in this flight, which was affected not only by regional fires but also by upwind fires in Mato Grosso and Rondonia.

Flight 12. Ozone concentrations were in the 60 ppbv level due to regional as well as upwind fires.

Without considering the size of fires, type of burned vegetation, combustion efficiency, and transport of pollutants, the above data indicate that ozone concentrations varied from 80 ppbv in regions with >10 fires/10,000 km^2 to 20 ppbv in regions with <5 fires/10,000 km^2. The results show a clear relation between the extent of biomass burning on a synoptic scale and the concentration of tropospheric ozone [*Cros et al.*, 1988].

TABLE 2. Fire Temperature and Burned Area Statistics Within 4° to 10°S and 48° to 60°W Around Alta Floresta
[After *Menzel et al.*, 1990]

Date	Time, UTC	Number of Fires	Apparent Fires Temperature, °K	Area Burning, km^2
Sept. 4, 1989	1349	10	452	16
	1649	45	522	37
	1831	30	510	19
Sept. 5, 1989	0149	0	...	0

5.3. *Trace Gas and Smoke Particles Emission*

5.3.1. *Method of calculations.* Emission factors were calculated using the carbon mass-balance (CMB) method to compute the mass of fuel that produced the emissions [*Ward et al.*, 1989; *Ward et al.*, 1982; *Nelson*, 1982]. The method is based on the stoichiometric partial oxidation of fuel ($C_6H_9O_4$) to CO_2 and incomplete combustion products. Carbon contained in the fuel is about 50% of the mass of the fuel [*Byram*, 1959], therefore the measured mass of carbon

TABLE 1. Summary of the Ozone Concentration Measurements During BASE-A in Transient Flights and Their Relation to Fires in the Vicinity of the Flight Path

Flight Number	Date	Time	Altitude m	Ozone ppbv	Fires in States Affecting the Flight: State	Number of Fires
1	Sept. 1	0840–1000	2700	40	Goias	7266
					São Paulo	184
					Minas Gerais	9344
					Mato Grosso do Sul	45
					Mato Grosso	1098
2	Sept. 2	0900–1120	1500	50–65	Goias	4187
3	Sept. 2	1240–1450		50–60	Tocantins	8479
7	Sept. 6	1200–1400	2400	55–65	Para	514
8	Sept. 6	1500–1630	1400	25	Amazonas	326
9	Sept. 6	1120–1315	1800	30–45	Amazonas	326
10	Sept. 7	1620–1720	3300	35–60	Rondonia	1142
					Mato Grosso	2922
11	Sept. 8	1440–1700	2200	60–80	Goias	1277
					Rondonia	282
					Mato Grosso	1640
12	Sept. 9	1830–1900	3400	55–60		

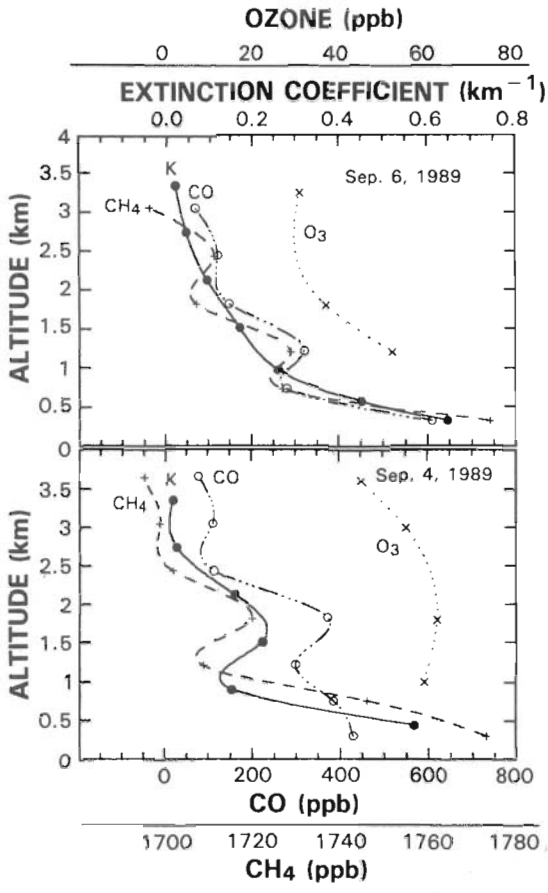

Fig. 4. Profiles of the CO (open circles), CH_4 (pluses), and ozone (crosses) concentrations and simultaneous extinction coefficient (solid circles) profiles at 0.45 μm (an optical measurement proportional to the particulate matter concentration). September 6, 1989, at 0830–0930 LST and September 4, 1989, at 1100–1200 LST.

contained in the combustion products is multiplied by 2 to calculate the mass of the consumed fuel in producing the combustion products. In order to verify the carbon concentrations in the biomass, nine samples of the more common fuels consumed by the fire were returned to the United States for analysis. The fuels consisted of stems, twigs, and leaves, which had an average carbon concentration of 53.4 ± 1.8%.

Emission factors for specific emission components are calculated by dividing the mass of the component by the fuel consumed and are expressed in units of grams of emission released per kilogram of fuel consumed (g/kg). Combustion efficiency is defined here as the mass of carbon released in the form of CO_2 divided by the total mass of carbon released.

5.3.2. *Emission factors and combustion efficiency.* The net concentrations of gases and particulate matter (after subtracting the background concentrations) were measured in three forest and one cerrado plume (Table 3). Background concentration data was averaged for a number of samples collected near the same altitude as the plume penetrations. Unlike the aged plumes sampled by *Andreae et al.* [1988] at concentrations near that of background, the particulate matter concentration of the ambient air was considered to be low relative to the in-plume concentrations.

The emission factors (Table 4) were calculated from the net concentrations (Table 3), using the CMB technique. The average emission factor for CO is 88 ± 30 g/kg for the three samples of smoke from fires for deforestation purposes. This emission factor compares very well with 91 ± 21 g/kg measured by *Hegg et al.* [1990] for forest fires in North America and the calculated emission factors of 91 g/kg from the data of *Andreae et al.* [1988] These emission factors are lower than those of *Ward et al.* [1989] from tower sampling of logging slash fires of 156 ± 37 g/kg for Douglas-fir slash and 128 ± 22 g/kg for hardwood species slash. The samples of *Hegg et al.* [1990] were collected in a similar way to this study. The measurements by *Ward et al.* [1989] were for the flaming and smoldering combustion phases and weighted for the entire fire based on the fuel consumed during each of the combustion phases. Emission factors for CH_4 from fires for deforestation averaged 4.8 ± 2.0 g/kg compared to the average by *Hegg et al.* [1990] of 2.9 ± 0.7 and that of *Ward et al.* [1989] of 5.5 ± 2.0 for Douglas-fir logging slash.

Particulate matter emission factors require a sample with a weighable mass of particles from a sample space concurrent with the collection of a sample of the gases. The gas concentrations must be accurately measured to differentiate them from the background concentrations. The large-bag sampling system enhances the collection from portions of the smoke plumes where the concentrations are differentiable from the background. PM2.5 emission factors ranged from 4 g/kg for the cerrado sample to 16 g/kg for one of the tropical deforestation fires.

The measured emission factors are plotted against the algorithms of *Ward and Hardy* [1991] as a function of combustion efficiency (Figure 5). The algorithms were developed from 38 test fires in the western United States and include numerous samples from both the flaming and the smoldering combustion phases. The combustion efficiency

TABLE 3. Net Concentration of Gases and PM2.5 for One Cerrado (Low Trees, Brush, and Grass Fuel Type) and Three Tropical Deforestation Fires Sampled From the INPE Aircraft Using Grab Sampling Techniques

Sample Concentration Date	Time, UT	Vegetation Type	Excess Concentration				Background		
			CO_2, ppmv	CO, ppmv	CH_4, ppmv	PM2.5, $\mu g/m^3$	CO_2, ppmv	CO, ppmv	CH_4, ppmv
Sept. 2, 1989	1058	cerrado	91	1.96	0.08	399	362	0.192	1.72
Sept. 3, 1989	1256	deforestation	129	11.88	1.04		354	0.268	1.71
Sept. 4, 1989	1500	deforestation	35	1.47	0.14	193	355	0.498	1.76
Sept. 7, 1989	1358	deforestation	10	1.12	0.12	177	363	0.643	1.76

PM2.5, particles with mean mass aerodynamic diameter of less than 2.5 μm. INPE is Instituto de Pesquisas Espaciais. For comparison the background concentrations are also given.

TABLE 4. Emission Factors for PM2.5, CO_2, CO, and CH_4 for a Cerrado and Three Deforestation Fires in Brazil During September 1989

Sample Combustion Date	Time, UT	Vegetation Type	Emission Factors, g/kg				Efficiency
			CO_2	CO	CH_4	PM2.5	
Sept. 2, 1989	1058	cerrado	1783	24	0.6	4	97
Sept. 3, 1989	1256	deforestation	1666	98	4.9	···	91
Sept. 4, 1989	1500	deforestation	1741	47	2.5	5	95
Sept. 7, 1989	1358	deforestation	1586	121	7.2	16	86

PM2.5, mass of particles < 2.5 μm in diameter.

for the cerrado fire was 97% and for the three tropical deforestation fires averaged 91 ± 4%. This compares to the measurements of *Hegg et al.* [1990] of 90 ± 2%, of *Andreae et al.* [1988] of 92% (as calculated from the CO/CO_2 molar ratio), and to the measurements of *Ward et al.* [1989] of 84 to 89% dependent on fuel type and burning conditions. The measurements of emissions from fires in tropical fuel types agree well with the measurements for fires in North America when plotted as a function of the combustion efficiency.

The ratios of emission factors as measured in the BASE-A experiment are summarized in Table 5 and are compared with similar measurements in North America and Brazil. It was found that although the fire combustion efficiency varied between the three observed fires, and as a result the ratio of CO/CO_2 varied (see the standard deviations in Table 5), the ratio of PM2.5 to CO or to CH_4 are markedly constant for deforestation fires. These ratios are compared in Table 5 and Figure 6 with similar ratios measured by *Ward* [1986] in North America. The variability in the North American data is much larger. Since only two forest fires were used to compute the ratio of particles to CO and CH_4 during BASE-A and three fires to study the ratios between the emitted trace gases, as compared to 38 fires in North America, it is difficult to reach a general conclusion. The small variability may be a result of the chance sampling of fires with similar characteristics. The ratio of CH_4 and CO, taken from Table 4, was measured in BASE-A in three forest fires resulting in 5.4 ± 0.4% which is also remarkably constant. The BASE-B results [*Ward et al.*, this issue] show good agreement with the preliminary findings for BASE-A (CO/PM2.5 ratios of 19 ± 8 and 14 ± 5 for the cerrado and forest areas, respectively). A constant ratio between PM2.5 and trace gas emissions is important for remote sensing of biomass burning from space (see section 2).

Radke et al. [1991] found that large biomass fires, capped with deep cumulus clouds (depth larger then 2 km), can produce significant scavenging of the particles. Since plume samplings reported in this paper were taken under the condensation level, scavenging could not affect the results shown in Table 5.

5.3.3. *Spiral profiles.* Profiles of the concentration of CO_2, CO, and CH_4 were made while ascending and descending through the atmosphere from 150 m to over 3500 m altitude 50 km west of Alta Floresta on September 4 and 6 at 1100 and 0830 LT, respectively. The CO and CH_4 profiles are compared with simultaneous measurements of the ozone concentrations and smoke particle extinction coefficients (Figure 4). In both cases the CO and CH_4 concentrations were maximal near the surface and decreased with altitude. In Figure 4 the early morning profile of September 6 appears smooth and exponential, where the profile for September 4 shows an abrupt increase in concentration at an altitude of 2 km. In this case, the profiles taken close to solar noon include smoke layers emitted directly to the higher altitudes by the new fires. The ozone and extinction coefficient profiles follow the same general pattern.

5.3.4. *Inorganic content of PM2.5.* The lightly loaded filters may have contributed to some of the differences between measurements of trace elements for samples collected in the cerrado and tropical deforestation fires and those for North America. Generally, the filter samples collected in the United States contain above 100 μg of sample per filter and often as high as 1 mg. The filter samples for Brazil contained 13 and 14 μg for the two deforestation fires and 29 μg for the cerrado fire.

Analysis of the inorganic content of the PM2.5 was done using X ray fluorescence techniques. Although the detection limit using the analysis technique for the lightly loaded filters may be questioned, the presence of Hg and the absence of lead is of special interest (Figure 7). Lead is generally considered to be a deposition product residual from leaded gasoline, and mercury was found for the tropical deforestation samples collected in the Amazon tropical forested areas but not the cerrado. The presence of mercury with the smoke particles may be a result of the widespread use of mercury to remove gold from ore in this region of Brazil. Of further interest is the high content of Si, Ca, Cl, and K for

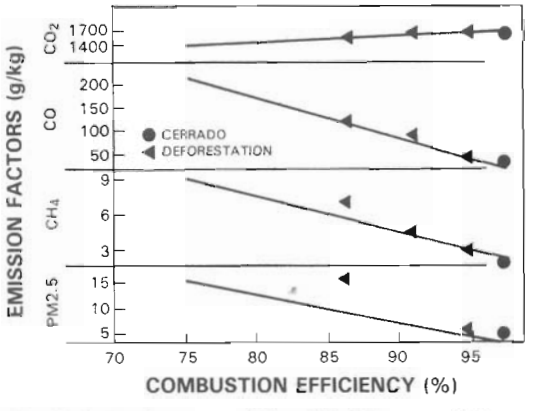

Fig. 5. Emission factors for CO_2, CO, CH_4, and PM2.5 (particulate matter for particles of diameter <2.5 μm) as functions of combustion efficiency. The data for the cerrado and tropical deforestation fires (symbols) are superimposed on the relation (solid line) derived for data for logging slash fires in the United States [*Ward and Hardy*, 1991]. The two groups of fires show similarity of emission factors for various emissions for different combustion efficiencies.

TABLE 5. Average Emission Ratios Measured During BASE-A From Cerrado and Deforestation Fires Compared to Previous Measurements in Brazil and North America of Emissions From Deforestation Fires

Parameter	BASE-A		*Crutzen and Andreae* [1990]	*Ward* [1986]		*Andreae et al.* [1988]	*Greenberg et al.* [1984]	*Radke et al.* [1990]
	Cerrado	Forest		Flaming	Smoldering			
				Percent on a Mass Basis				
CO/CO2	1.4	5.4 ± 2	6.6	4.3 ± 1.6	18 ± 9	5.4	3–20	5.3 ± 2.4
CH4/CO2	0.03	0.3 ± 0.1	0.6	0.1 ± 0.1	0.5 ± 0.2	0.2–0.8	0.19 ± 0.08	
Particles/CO2	0.25	0.6 ± 0.3*	0.8	0.4 ± 0.3	0.8 ± 0.3	0.15–0.6†	0.95 ± 0.36	
Particles/CO	18	12 ± 0.8*	12	9.6 ± 3.5	5.6 ± 2.3		19 ± 6	
Particles/CH4	786	215 ± 2*	200	325 ± 183	177 ± 63		580 ± 260	
Graphitic Carbon/particles	3.3	10.0 ± 3.0*	11‡			9§		
Combustion efficiency	97	91 ± 4		92 ± 3	77 ± 7			

*The uncertainty was computed as half of the measured variation between the two measurements in Table 4.
†Computed as a product of TPM/kg C, ratio of volume of submicron particles to total particles and ratio of carbon to total fuel mass from *Andreae et al.* [1988].
‡Computed as a product of the ratio of EC/TPM in mole ratio and ratio of the weight of C in TPM and the total weight of TPM.
§Computed as a product of the ratio of EC/POC of 0.13 and the ratio of POC/TPM of 0.66 from *Andreae et al.* [1988].

the cerrado area. The S and Cl are in low concentration for the tropical deforestation smoke relative to the smoke from the cerrado fires. Future analyses of the elemental composition of the biomass fuels should help explain these differences between the inorganic elemental composition of the fuel types in Brazil as well as the differences between typical smoke samples collected in other parts of the world.

5.3.5. *Carbon content of PM2.5.* Analysis of the carbon content of smoke particles smaller than 2.5 μm in diameter (PM2.5) was made using a volatilization/combustion technique of *Johnson and Huntzicker* [1981]. The ratio of graphitic to organic carbon measured with the technique was considered to be valid even though, in this technique, some mass of carbon is lost from the sample. The ratio of graphitic to organic carbon was found to be 3 times lower for the smoke in the cerrado than for the smoke from tropical deforestation fires (Table 5). The results are compared to carbon ratios measured for fuels in the United States and Canada (Figure 8).

5.4. *Optical Measurements of Smoke Particles*

5.4.1. *Method of calculations.* The aerosol optical thickness in each spectral band (defined as the absolute value of the natural logarithm of the vertical transmission) is computed from the Bouguer-Lambert-Beer law

$$V_\lambda = r^2 V_{0\lambda} \exp(-\tau_\lambda/\mu_0) \quad (2)$$

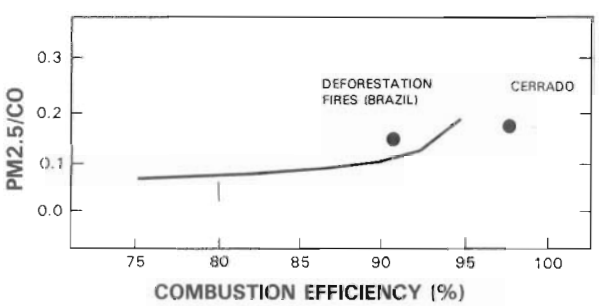

Fig. 6. The ratio of mass of PM2.5 to CO for fires in the United States (solid curve) and the average ratio for the tropical deforestation and cerrado fires (solid circles) as a function of combustion efficiency.

where V_λ is the output voltage of the sunphotometer for a bandwidth λ; $V_{0\lambda}$ is the zero air mass voltage intercept at that band pass for a mean normalized Earth-Sun distance (r) of 1.00; τ_λ is the wavelength dependent vertical optical depth above the sunphotometer; and μ_0 is the cosine of the solar zenith angle at the observation site.

The wavelength dependence of the aerosol optical thickness is a measure of the particle size distribution [*King et al.*, 1978]. It may be expressed in terms of the Angstrom exponent α [*Kaufman and Fraser*, 1983],

$$\alpha = -\frac{\ln(\tau_2/\tau_1)}{\ln(\lambda_2/\lambda_1)} \quad (3)$$

where λ_1 and λ_2 can be any two "aerosol" spectral channels. Optical measurements are sensitive mainly to particles in the accumulation mode [*Whitby*, 1978; *Kaufman and Fraser*, 1983], which for smoke particles can be described by a lognormal function [*Radke et al.*, 1978; *Stith et al.*, 1981; *Andreae et al.*, 1988]. Therefore instead of a common relation between α and a power law size distribution, a lookup table of α was computed using Dave's Mie scattering code [*Dave and Gazdag*, 1970] as a function of the size distribution parameters (mean geometric radius, r_g, and the geometric standard deviation of the distribution). For the hygroscopic organic particles, for a relative humidity of 70%, we assumed a refractive index of 1.43–0.0035i [*Kaufman et al.*, 1990*a*]; r_g was converted to the effective radius r_{eff} according to

$$r_{\text{eff}} = r_g \exp(2.5\sigma^2) \quad (4)$$

where $\sigma = \ln \sigma_g$ and σ_g is the geometric standard deviation.

The effective radius r_{eff} is defined as the ratio of the volume and the geometrical cross section

$$r_{\text{eff}} = \frac{\int_0^\infty r^3 n(r)\, dr}{\int_0^\infty r^2 n(r)\, dr} \quad (5)$$

It is an appropriate parameter for radiative computations. The advantage of r_{eff}, in contrast with r_g, is that once $\tau(\lambda)$ is

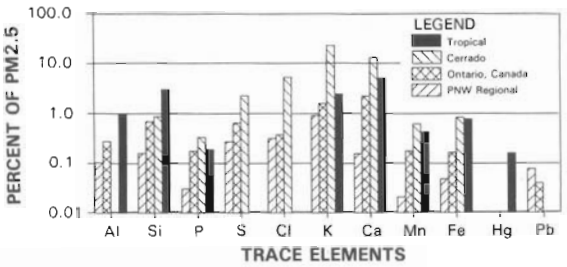

Fig. 7. Inorganic content of PM2.5 for the cerrado and tropical forest deforestation fires as compared to a fire in Canada and the average of 38 test fires in the Pacific Northwest (PNW), United States.

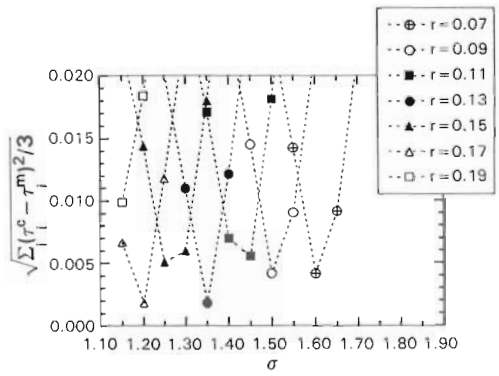

Fig. 9. Sum of the differences between the retrieved optical thickness τ^c and the measured optical thickness τ^m for three bands (0.45, 0.65, and 0.85 μm) plotted as a function of the standard deviation σ for several mean geometric radii.

computed for a given r_{eff}, it does not have a strong residual dependence on σ. The analysis of the data showed that the spectral range of the present optical thickness observations (at wavelengths of 0.45 to 0.85 μm) is not wide enough to measure σ (see Figure 9). Therefore in the rest of the paper the results for r_{eff} will be given for a range of σ between 0.3 and 0.9. This range was chosen based on the size distributions measured from aircraft by *Radke et al.* [1978] and *Stith et al.* [1981]. It introduces an uncertainty in r_{eff} of ± 0.3 μm (see Table 7 for example).

5.4.2. *Ground-based observations.* Sunphotometer measurements were conducted on September 3, 4, and 6, in 1989, during prescribed fire events near Alta Floresta, Matto Groso, in Brazil. Ground observations of mixed smoke were made in the mornings before the fires were started. Plume observations were made from flaming and smoldering conditions and in the case of the flaming source, observations from 10 m, 500 m, 1 km, and 10 km from the source allowed evaluation of the effects of short-term aging on the aerosols.

Mixed smoke observations: Mixed smoke observations are made away from the plume on all observation days. These measurements represent local background conditions and can be used to extract the smoke properties of a particular plume from the total measurements of the optical thickness. The mixed smoke optical depth increased from morning through the afternoon at all wavelengths due to the increase of emission products introduced to the mixing layer from biomass burning. The spectral dependence of the optical thickness, α (in (3)), increased during the day from 1.5 to 2.2, indicating a decrease in the effective particle radius from 0.45 to 0.22 μm, from the aged morning smoke to the fresher afternoon smoke (Figure 10). The optical depth of the mixed smoke increases from September 3 through 6, however, the trend was small and did not affect α or the derived value of r_{eff}. We therefore used the smoothed time dependent values for all dates as background values to be subtracted from individual plume observations and result in the net plume optical thickness.

A second correction for the measured plume optical thickness was made by subtracting the optical thicknesses measured by the aircraft above 4 km. These high-level atmospheric optical thicknesses were shown to be relatively

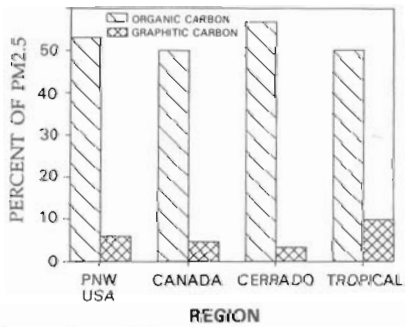

Fig. 8. Comparison of the organic carbon content of the emissions of PM2.5 for fires of the cerrado and tropical areas as compared to a fire in Canada and the average of 38 fires in the Pacific Northwest (PNW), United States.

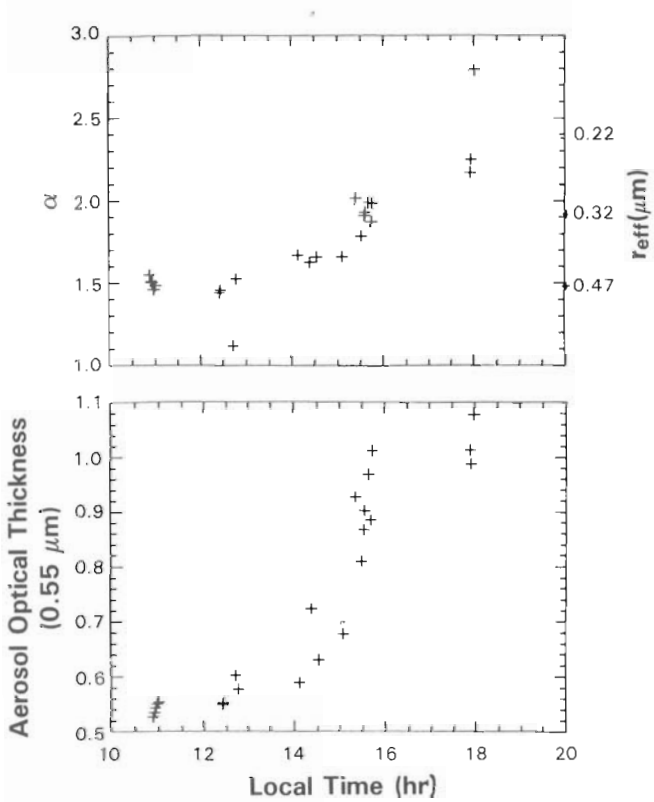

Fig. 10. Sunphotometer observations made during September 3 and 4, 1989, of the optical thickness (τ) for (bottom) 0.55 μm and (top) its spectral dependence (α) for background mixed smoke conditions as a function of the time of the day. The corresponding effective particle radius (r_{eff}) is also given.

TABLE 6. Summary of Ground-Based Measurements

Smoke Type	Plume Values		r_{eff}		
	τ_a(0.50 μm)	α(0.50/0.875)	Whole Atmosphere	Mixing Layer	Plume
Fresh smoke, 10 s	1.0–1.7	2.4 ± 0.3	0.20–0.27	0.13–0.22	0.14–0.24
Less fresh smoke, 1 min	1.0–2.1	2.8 ± 0.2	0.19–0.20	0.12–0.15	0.10–0.15
Less fresh smoke, 5 min	0.45–0.75	3.15 ± 0.05	0.20–0.22	0.11–0.15	0.07–0.09
Aged smoke, 1 hour	1.0–1.1	2.85 ± 0.03	0.19–0.20	0.12–0.15	0.11–0.12
Mixed smoke	0.5–1.0	1.5–2.2	0.22–0.45*		

For τ_a(0.64 μm), the aerosol optical thickness; α(.50/.875), the wavelength dependence of the optical thickness; and r_{eff}, the effective radius of the particles.
*Observations taken over a range of days and burning conditions.

stable through time. This resultant optical thickness characterizes a combination of the plume and mixing layer. We therefore analyzed observations of smoke from active fires in three conditions termed "whole atmosphere," "mixing layer," and "plume." These were analyzed for flaming and mixed smoke conditions.

Fresh smoke from flaming fires: Observations of fresh smoke (approximately 5 to 10 s old) from flaming fires were highly variable due to the lack of homogeneity of the plume during the 40 s required to make a spectral observation series. A running average of 20 observations out of the 80 observations collected continuously from a specific fire decreased the high-frequency variations in the wavelength dependence of the optical thickness. No further increase in stability was noted by averaging on a larger number of observations. The results are summarized in Table 6. The effective radius r_{eff} of the fresh smoke in the plume is r_{eff} = 0.14 to 0.24 μm (for σ = 0.5 and corresponding to α = 2.1 to 2.7), the mixing layer results in r_{eff} = 0.13 to 0.22 for the plume plus boundary layer smoke, and r_{eff} = 0.20 to 0.27 for the whole atmosphere.

Two other data sets of slightly older smoke (~1 and ~5 min) were analyzed in the same way. The wavelength exponent for the plume increased with aging time from 2.4 for fresh smoke to 2.8 and 3.2 for 1-min and 5-min-old plumes, respectively, with a corresponding decrease in the value of r_{eff} for the net plume from 0.19 to 0.13 μm and 0.08, respectively (Table 6). Observations of 1-hour aged plume, approximately 10 km downwind of the source, showed a decrease in the wavelength exponent to 2.85, with a corresponding smaller particle size r_{eff} = 0.11.

Discussion of the ground-based observations: The sunphotometer measurements showed the difference between mixed aged smoke and fresh smoke. Aging of the smoke in the first 1 hour decreased the effective radius for the mixed layer for flaming fires from 0.17 to 0.13 μm (see the average of the first and last line in Table 6 for the mixed layer). The decrease of the particle size within the first 1 hour can be attributed to the deposition of larger ash particles generated in the dynamic flaming fires but not during smoldering. The increase in the particle size in the next several hours (from the fresh smoke to the mixed aged smoke measured the next morning) can be due to coagulation of the liquid organic aerosol particles and interaction with water vapor. The smoke aerosol model, which is applicable for remote sensing of fresh biomass burning, is therefore defined by a particle mean mass radius between 0.10 and 0.20. The mixed aged smoke model would be represented by a mean mass particle radius of 0.2 to 0.4 μm. For comparison, aircraft measurements of volume size distribution of fires in North America made by *Radke et al.* [1978] and *Stith et al.* [1981] showed mean mass radii between 0.12 and 0.22 μm, which is similar to the present measurements. *Radke et al.* [1991] found that the mean mass radii of particles in the accumulation mode is 0.16 μm for fresh smoke, increasing with the particle aging due to coagulation. *Andreae et al.* [1988] measured the size distribution of smoke particles in Brazil and also found that the maximum concentration of the accumulation mode is around 0.12 μm radius.

5.4.3. *Airborne observations of water vapor profiles*. Three water vapor profiles from September 3, 4, and 6 indicated almost identical results (Figure 11). Approximately 50% of the total water vapor is within the first kilometer. Above 3 km the total precipitable water vapor is less than 0.5 cm. Because the mixing layer was below 3 km throughout the experiment, virtually all of the water in the atmosphere is available for interaction with the emission products. Note that on September 6 the artificially high concentration of water vapor at 0.6 km is due to the presence of thin cirrus clouds that happened to be present during the measurement and increased the apparent differential water amount and extinction at 0.6 km (that are computed from the differences between the total water vapor and optical thickness, respectively, at two altitudes) and as a result decreased it at 0.3 km.

5.4.4. *Airborne observations of aerosol profiles*. Three

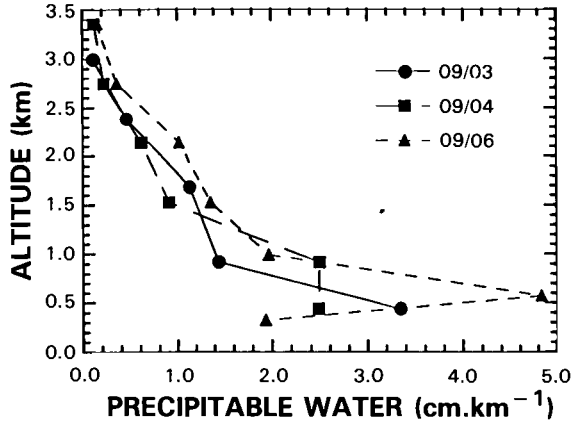

Fig. 11. Vertical profile of the precipitable water for three dates and different time of day for September 3, 1989, 1500 LST; September 4, 1989, 1200 LST; and September 6, 1989, 1000 LST.

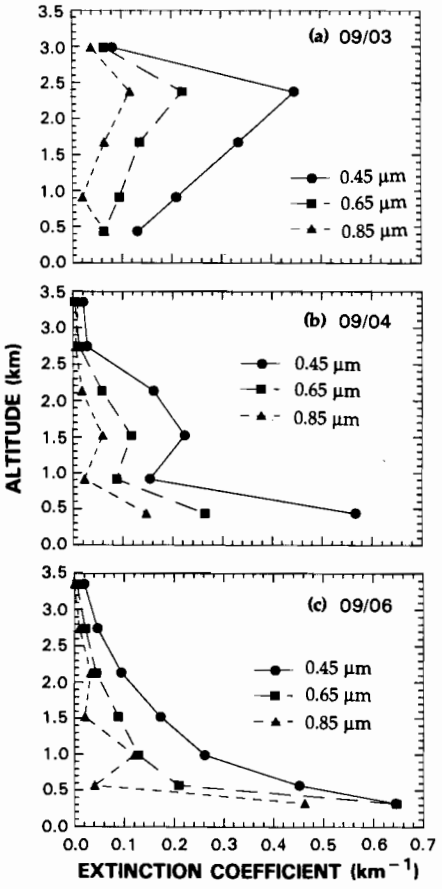

Fig. 12. Vertical profiles of the extinction coefficient measured at 0.45, 0.65, and 0.85 μm for September 3, 1989, 1500 LST; September 4, 1989, 1200 LST; and September 6, 1989, 1000 LST.

aerosol profiles were measured corresponding to 3 times of the day (Figure 12): a morning, 1000 LST flight (September 6); a 1200 LST noon flight in which the mixing layer is becoming active but with only aged (>1 day) smoke and smoke from smoldering (September 4); and an afternoon, 1500 LST profile in which many flaming fires are contributing to the aerosol loading (September 3). The morning profile resulted in large extinction coefficients (>0.5 km^{-1}) for all wavelengths below 500 m above ground level (agl). The extinction coefficients decreased exponentially with elevation to less than 0.1 km^{-1} above 2.0 km agl (Figure 12*c*).

The noon profile (Figure 12*b*) indicated high extinction coefficients below 0.5 km and between 1.5 and 2.0 km with a much stronger wavelength dependence than the morning profile. Above 2.5 km the results were very similar to the morning profile (Figure 12*c*). The afternoon profile (Figure 12*a*) showed emission from the flaming smoke directly to a layer at 2 to 3 km agl. Thin high smoke layers were already observed in Brazil during the burning season [*Andreae et al.*, 1988]. In contrast to the other profiles the lowest extinction coefficients occurred near the ground and like the other profiles almost no wavelength dependence was observed for the highest layer (>3 km, Table 7).

The mean optical thickness above 3.5 km was comparable in the three days of observations: 0.13 ± 0.02 at $\lambda = 0.65$ μm (Table 7). It was less wavelength dependent in the morning conditions than in the noon or afternoon conditions; the corresponding effective radius r_{eff} decreased from more than 1 μm for morning conditions to 0.5 μm for afternoon conditions. The aerosol optical thickness of the mixing layer was in the range of 0.25 to 0.36 at 0.65 μm. The effective radius was the largest in the morning (0.22) and decreased as a function of time toward the afternoon. These results confirm the smaller particle size for fresh smoke, emitted in the afternoon, as deduced from ground measurements.

In Figure 4 the September 6 morning extinction coefficient profile at 0.45 μm was plotted against the CO, CH_4, and O_3 profiles. These four profiles demonstrate an exponential decrease in value with elevation over nearly an order of magnitude of change of CO and particulate matter concentration (or extinction). The ozone concentration is offset by 30 ppbv from the high-altitude background value. The noon profile (September 4) also demonstrated a high degree of similarity. This relationship among the CO, CH_4, ozone, and particulate matter profiles shows the cause and effect relation between emissions from biomass burning and the atmospheric concentration of trace gases. Because of the elevated concentrations of the smoke particles it is reasonable to conclude that the measured CO concentrations of 600 ppbv and the additional CH_4 and ozone concentration above the background values are generated directly (CO and CH_4) or indirectly (ozone) by biomass burning. High concentrations of CO and ozone in smoke plumes from biomass burning were also reported by *Andreae et al.* [1988]. These results suggest that remote sensing of the optical properties of the aerosols can potentially be a good estimator of CO and CH_4 emissions and of the elevated ozone concentrations under these conditions. In order to develop the potential of the remote sensing technique the relation between trace gases

TABLE 7. Smoke Aerosol Optical Thickness, τ, Wavelength Dependence, α, and Particle Effective Radius, r_{eff}, for the Mixing Layer and the Layer Above 3.5 km From Aircraft Measurements

Date	Time, LST	τ, 0.45 μm	τ, 0.65 μm	τ, 0.85 μm	α	r_{eff}, μm
			Layer Above 3.5 km			
Sept. 9, 1989	1500	0.17	0.12	0.10	0.83	≈0.5
Sept. 4, 1989	1200	0.16	0.15	0.14	0.21	≈1.0
Sept. 6, 1989	1000	0.13	0.12	0.11	0.26	≥1.0
			Mixing Layer			
Sept. 3, 1989	1500	0.76	0.36	0.18	2.26	0.16 ± 0.03
Sept. 4, 1989	1200	0.55	0.26	0.12	2.40	0.20 ± 0.03
Sept. 6, 1989	1000	0.57	0.31	0.16	2.00	0.22 ± 0.03

and particulates have to be measured repetitively across the biomass burning regions. A first attempt in this direction was taken by *Ward et al.*, this issue].

5.4.5. *Single scattering albedo and graphitic carbon.* The single scattering albedo measures the effectiveness of the aerosol absorption and depends on the refractive index and on the size distribution of the particles. Smoke aerosol is composed of organic material and graphitic carbon. Since it is not clear what the mixture between these two substances in the smoke particles is, e.g., if the graphitic carbon is in the form of separate particles or serves as the nucleus for the condensation of the organic material, it is assumed here that the graphitic carbon particles are mixed with organic particles in an external mode. If instead of assuming an external mode, it would have been assumed that the graphitic carbon particles are located in the center part of the smoke particles, then the absorption values would have been twice as large [*Ackerman and Toon*, 1981]. Graphitic carbon has a refractive index of $2.00–0.66i$ [*Ackerman and Toon*, 1981]. For the organic particle characteristics we assumed a refractive index of $1.43–0.0035i$ [*Kaufman et al.*, 1990*a*]. The particle effective radius is 0.03 to 0.10 for graphitic carbon [*Ackerman and Toon*, 1981] and 0.15 for organic particles (see section 5.4.2).

During the BASE-A experiment, mass measurements were made only through the plume of smoke generated in the flaming phase and 10% of the total mass was found to be graphitic carbon (Table 5). For 70% relative humidity, liquid water consists 50% of the particles volume [*Hänel*, 1981; *Fraser et al.*, 1984; *Kaufman et al.*, 1990*b*]. Therefore graphitic carbon consists 5% of the total particles mass. For simplicity the volume ratio was assumed identical to mass ratio. For three intermediate mass radii within the previous range (0.03, 0.05, and 0.10 μm), we computed the single scattering albedo from the Mie theory by assuming an external mixing between the organic and the graphitic carbon. The results are within the range of 0.89 to 0.91 (similar to finding of *Kaufman* [1987] for North American fires) but more absorbing than indicated from remote sensing studies (0.97 by *Kaufman et al.* [1990*a*, *b*]). Internal (rather than external) mixture between the graphitic carbon and the nonabsorbing part of the smoke aerosol would result in a lower value of the single scattering albedo [*Ackerman et al.*, 1981], though a lower value would be inconsistent with remote sensing studies [*Kaufman*, 1987]. Since the mass ratio of graphitic carbon was measured through the plume only, it seems reasonable to assume that the single scattering albedo would be larger far away from the fire. *Radke et al.* [1991] noticed that smoke processed through a cloud increases in brightness. One possible explanation, suggested by *Radke et al.* [1991], is that the aggregate chains of graphitic carbon collapse, while at the same time the number of particles decreases, resulting in larger-size particles and lower absorption. *Radke et al.* [1991] measured the single scattering albedo of smoke particles in North American fires by measuring light extinction with an optical extinction cell and light scattering with a nephelometer. They found that the average value of the single scattering albedo for 15 fires is $\omega_0 = 0.83 \pm 0.11$. This value is lower than values of ω_0 derived for the smoke in Brazil. Additional measurements (with different techniques) in the tropics and in North America are needed to establish this value and possible difference between the two fire regimes.

6. SUMMARY AND APPLICATION TO SATELLITE REMOTE SENSING

6.1. *Summary*

In the BASE-A experiment, emission measurements were performed from the INPE instrumented aircraft and from the ground of smoke particles, emitted trace gases (CO and CH_4), and subsequently produced ozone. The emission measurements were performed simultaneously with measurements of the optical properties of the smoke particles. Extensive ground measurements of the smoke particle optical thickness and effective size were conducted in the vicinity of Alta Floresta. Though only a limited number of measurements of trace gases and particles were made during the experiment, with only one plume penetration in the cerrado fire, three plume penetrations in the deforestation area, and two simultaneous profiles of trace gases, ozone, and smoke particle concentration, some general conclusions are possible. Additional measurements are a subject of further study [*Ward et al.*, this issue].

Relationship among CO, CH_4, ozone, and the extinction coefficient. In the two profiles, in which measurements of ozone, smoke particles, CH_4, and CO were taken simultaneously during BASE-A, a strong resemblance was found among the concentrations of ozone, CO, CH_4, and the smoke particle extinction coefficient. This relationship shows that biomass burning strongly contributes to the atmospheric concentration of particles and trace gases which enhances the production of tropospheric ozone. This relationship also indicates that satellite remote sensing of smoke particles has the potential to be used to detect the presence of the emitted trace gases and the produced ozone. Strong resemblance between CO and ozone profiles in the Amazon basin was also found by *Andreae et al.* [1988].

Relationship between fires and ozone. A strong relationship was found between the spatial distribution of fires across the Brazilian Amazon basin and the ozone concentration. The ozone concentration increased from 20 to 30 ppbv in regions with less than five fires per 10,000 km^2 to 70 to 80 ppbv in regions with more than 10 fires per 10,000 km^2. This relationship also shows that biomass burning has a decisive role in the formation of elevated levels of tropospheric ozone in the Amazon basin during the dry season. High ozone concentration downwind from fires in Africa were reported by *Andreae et al.* [1992].

Aerosol particles as a tracer of biomass burning. In the two deforestation smoke plume tests, in which the concentrations of trace gases were measured simultaneously with in situ sampling of smoke particles, it was found that the ratio between the emitted smoke particles and trace gases such as CO and CH_4 varied much less than the ratio between CO_2 and CO or CO_2 and CH_4. This relationship is much better than that for fires measured in North America (see Table 5). Though the stability of the ratio between the emitted particles and trace gases was determined only for two fires, it can be expected from theoretical considerations. The nearly constant ratio of CO and CH_4 to particles, and the variable ratio to CO_2, is due to the similarity in the combustion processes that generate these species. The mass loading of the biomass and the fraction of the burned material affects particle emissions as well as the emissions of trace gases including CO_2. But the combustion efficiency determines the rate of emission of particles and trace gases other than CO_2,

TABLE 8. Upward Radiance, in Reflectance Units, $\pi L/F_0\mu_0$, and Corresponding Optical Thicknesses Measured From the Aircraft on September 6, 1989, for Two Flight Altitudes

Wavelength μm	Measured Radiance		Measured Aerosol Optical Thickness	
	500 m	3500 m	500 m	3500 m
0.44	0.015 ± 0.004	0.067 ± 0.005	0.62	0.13
0.65	0.018 ± 0.005	0.039 ± 0.005	0.35	0.12

at the expense of CO_2 emissions. Therefore remote sensing of smoke particles is a direct measure of the emission of trace gases, accounting for the biomass loading and the fraction of the burned material. Furthermore, since the gases CO and CH_4 are produced proportionally to the production of particles (on a mass basis), the remote sensing of particles accounts for variations in combustion efficiency. The relationship between the division of the carbon mass between the products of incomplete burning (particulates, CO, CH_4, etc.) cannot be established solely based on the present limited data. It is a subject of ongoing measurements [*Ward et al.*, this issue].

Fire combustion efficiency and emission ratios. Fire combustion efficiency in the tropics was found to be higher than for North American fires. As a result, less particles, CO, and CH_4 are released per unit mass of biomass burned. The rate of emission of trace gases and particles for a given combustion efficiency is similar in the tropics to the North American fires. In the cerrado the single sampled fire indicates that the emission is 5 to 10 times lower than the emission from tropical or North American forests.

Spectral optical thickness and the particle size. Spectral measurements from the ground and from aircraft of the smoke aerosol optical thickness indicate large Angstrom coefficients of α = 2.1 to 3.1 except for the upper troposphere (above 3.5 km), as measured from the aircraft and for smoke during morning conditions when the smoke was emitted at least one day earlier (α = 0 to 1.5). These results are in agreement with measurements conducted in North America from aircraft [*Pueschel et al.*, 1988] and lidar backscattering in Brazil [*Browell et al.*, 1990]. Assuming a lognormal distribution of smoke particles, with σ in the range 0.3 to 0.9, the effective radius r_{eff} for flaming fire plumes is in the range 0.10 to 0.18 for fresh smoke and 0.2 to 0.4 for mixed aged smoke. The inferred particle size distribution is similar to in situ measurements in North America [*Radke et al.*, 1991].

6.2. *Application to Radiance Measurements*

In this section the smoke particle optical model is used to predict the difference between the upward radiance measured below the smoke layer and at the top of the smoke layer. The radiance measurements were made above a uniform undisturbed forest on September 6, 1989, while simultaneously measuring from the aircraft the aerosol spectral optical thickness. The radiance measurements were taken at 500 and 3600 m above the ground in two spectral bands using a radiometer. The radiometer was calibrated in NASA/Goddard Space Flight Center calibration facility using an integrating sphere. Table 8 summarizes the differences in the radiances and optical thicknesses between 3600-m and 500-m altitude. The radiance values (L) are normalized to reflectance units ($\pi L/F_0\mu_0$, where F_0 is the extraterrestrial solar flux and μ_0 is cosine of the solar zenith angle).

Since the low-level radiance was measured at 500 m rather than at the ground, the difference in the measured optical thickness at 500 and 3500 m (also shown in Table 8 for two wavelengths) was used to compute r_{eff} for this smoke layer for two values of the width of the size distribution, σ. For each of the σ values the optimum value of r_{eff} was derived from the spectral optical thickness (see Table 9) and used to compute the difference in the upward radiance. The radiance computations are based on the assumption that the particles are spherical and have a lognormal size distribution. The radiances are mainly affected by the accumulation mode particles, which originate from condensation of hydrocarbons, and were found to be typically spherical [*Radke et al.*, 1991]. For both values of σ the same value of r_{eff} was obtained. Surprisingly though, the measured values of the radiance difference was not reproduced for σ = 0.5 but rather for σ = 0.2. This may be an indication that the wavelength dependence of the radiance is much more sensitive to the width of the size distribution than the wavelength dependence of the optical thickness and that the width of the size distribution of particles emitted from biomass burning in the tropics is much smaller than the width of the distribution measured from fires in North America.

Profiles of the upward radiance (in reflectance units) are plotted in Figure 13 and compared with model predictions. The model is based on radiative transfer computations using smoke particle parameters from simultaneous measurements discussed earlier in the paper: (1) aerosol optical profile given in Figure 12, (2) lognormal particle size distribution with effective radius r_{eff} = 0.22 (Table 7) and standard deviation of ln r of σ = 0.6, (3) single scattering albedo ω_0 = 0.9 (see section 5.4.5), and (4) refractive index 1.43–0.0035i.

The results show that the computed radiances are generally similar to the measured values. Measured radiances are higher for intermediate altitudes than the theoretical values, mainly in the shortest wavelength. A very good fit between theory and measurements is obtained for r = 0.65 μm.

7. CONCLUSIONS

Simultaneous measurements, during the Biomass Burning Airborne and Spaceborne Experiment in the Amazonia, of CO, CO_2, CH_4, particle mass and size, and their optical

TABLE 9. Comparison Between the Measured Radiance Difference Between the Two Flights and the Computed Radiance Difference for the Measured Optical Thickness and Several Values of the Effective Radius and the Width of the Particle Size Distribution σ That Fit the Measured Wavelength Dependence of the Optical Thickness

		Difference in the Upward Radiance			
		Measured		Computed	
r_{eff}	σ	0.44 μm	0.65 μm	0.44 μm	0.65 μm
0.17	0.20	0.047	0.018	0.047	0.017
0.17	0.50	0.047	0.018	0.058	0.027

The radiance (L) is given in reflectance units.

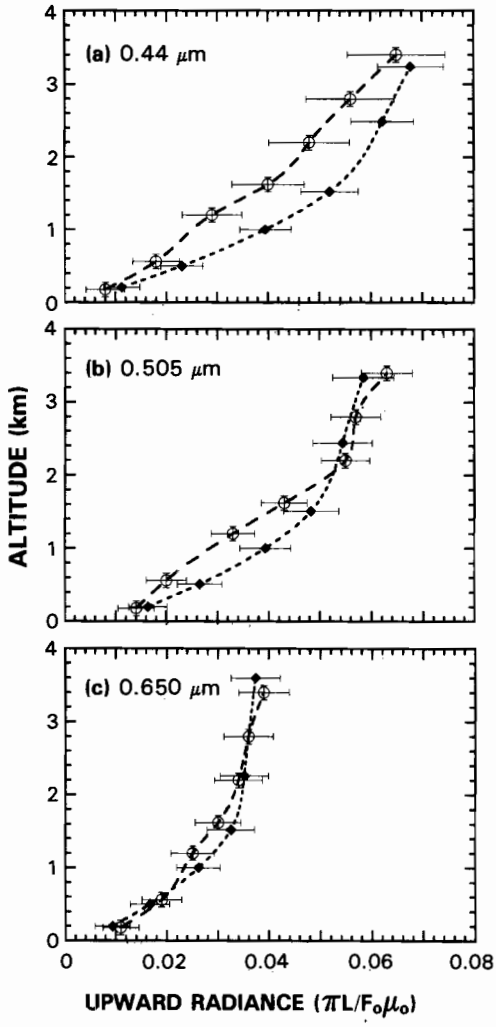

Fig. 13. Vertical profiles of the upward radiance (normalized to reflectance units) measured at three spectral bands from the aircraft on September 6 and the model predictions. The model is based on smoke particle characteristics measured during the experiment. Solid symbols, measurements; open symbols, theory.

properties, show similar emission ratios to measurements in North America. The main differences are of higher combustion efficiency in the Amazonia (97% in the cerrado and 90% for forest fires) and more stable ratios between emission species of products of incomplete combustion (e.g., CO, CH_4, and particulate matter). The higher combustion efficiency for the fire sampled in the cerrado resulted in 5 to 10 times lower emission factors than those from typical tropical or North American forest burns. Since only one fire was sampled in the cerrado, the results are not definitive and are the subject of further studies [*Ward et al.*, this issue], but they may indicate that the contribution of grassland fires to global emission of CO and CH_4 is smaller than expected. The correlations found among profiles of ozone, CO, CH_4, and particles show the direct link of biomass burning to elevated levels of ozone. The spatial relationship between the presence of fires and ozone across the Amazonia strengthen this conclusion. The measured optical characteristics of smoke from biomass fires and the relation between trace gases and particles form a basis for the development of techniques for remote sensing of biomass burning from space. The optical characteristics of the smoke particles, reported in this paper, are based on extensive measurements from the ground. The emission factors were based on four plume penetrations and two vertical profiles. Because of the sparcity of data for fires in South America the emission factors can be considered as preliminary and should be used in conjunction with the much larger data base from North America. There is a need to perform similar measurements in the future in several regions in the tropics where biomass burning takes place. There is also a need to measure the emissions from single fires as a function of time to establish the relative contribution of smoldering and flaming to the emissions and to average the emission factors on the whole fire cycle.

Acknowledgments. The authors wish to thank Alfredo C. Pereira, Pedro C. D. Santos, Luiz F. Ribeiro, Luiz M. N. L. Monteiro, and the DOP/INPE-C.P. operators for their collaboration in different parts of this work. We would also like to thank V. W. J. H. Kirchhoff and his group for the calibration of the ozone photometric analyzer and for the reduction of the ozone data. Support was partially provided by Fundacao Banco do Brasil through "Our Nature" and INPE's Amazonia Program, as well as by NASA/GSFC Directors' discretionary funds. We appreciate the extensive review by Wei Mei Hao and an anonymous reviewer.

REFERENCES

Ackerman, T. P., and O. B. Toon, Absorption of visible radiation in atmosphere containing mixtures of absorbing and nonabsorbing particles, *Appl. Opt.*, *20*, 3661–3668, 1981.

Albrecht, B. A., Aerosol cloud microphysics and fractional cloudiness, *Science*, *245*, 1227–1230, 1989.

Andreae, M. O., et al., Biomass burning emissions and associated haze layers over Amazonia, *J. Geophys. Res.*, *93*, 1509–1527, 1988.

Andreae, M. O., A. Chapuis, B. Cros, J. Fontan, G. Helas, C. Justice, Y. J. Kaufman, A. Minga, and D. Nganga, Ozone and Aitken nuclei over equatorial Africa: Airborne observations during DECAFE 88, *J. Geophys. Res.*, *97*(6), 6137–6148, 1992.

Browell, E. V., G. Gregory, R. C. Harris, and V. W. J. H. Kirchhoff, Tropospheric ozone and aerosol across the Amazon basin, *J. Geophys. Res.*, *93*(D2), 1431–1451, 1988.

Browell, E. V., C. F. Butler, P. Robinette, S. A. Kooi, M. A. Fenn, and S. Ismail, Airborne lidar observations of aerosols and ozone in plumes from biomass burning over the Amazon basin and over Alaska, paper presented at Chapman Conference on Global Biomass Burning, AGU, Williamsburg, Va., March 19–23, 1990.

Byram, G. M., Combustion of forest fuels, in *Forest Fire: Control and Use*, edited by K. P. Davis, pp. 61–89, McGraw-Hill, New York, 1959.

Coakley, J. A., Jr., R. D. Cess, and F. B. Yurevich, The effect of tropospheric aerosol on the earth's radiation budget: A parameterization for climate models, *J. Atmos. Sci.*, *40*, 116, 1983.

Coakley, J. A., Jr., R. L. Borstein, and P. A. Durkee, Effect of ship stack effluents on cloud reflectance, *Science*, *237*, 953–1084, 1987.

Cros, B., R. Delmas, D. Naganga, B. Clairac, and J. Fontan, Seasonal trends of ozone in equatorial Africa: Experimental evidence of photochemical formation, *J. Geophys. Res.*, *93*, 8355–8366, 1988.

Crutzen, P. J., Tropospheric ozone: An overview, in *Tropospheric Ozone*, edited by I. S. A. Isaksen, pp. 3–32, 1988.

Crutzen, P. J., and M. O. Andreae, Biomass burning in the tropics: Impact on atmospheric chemistry and biogeochemical cycles, *Science*, *250*, 1669–1678, 1990.

Crutzen, P. J., L. E. Heidt, J. P. Kranec, W. H. Pollock, and W. Seiler, Biomass burning as a source of the atmospheric gases CO, H_2, N_2O, NO, CH_3Cl, and COS, *Nature*, *282*, 253–256, 1979.

Crutzen, P. J., A. C. Delany, J. Greenberg, P. Haggenson, L. Heidt, R. Lueb, W. Pollock, W. Seiler, A. Wartburg, and P. Simmerman, Tropospheric chemical composition measurements in Brazil during the dry season, *J. Atmos. Chem.*, *2*, 233–256, 1985.

Dave, J. V., and J. Gazdag, A modified Fourier transform method

for multiple scattering calculations in a plane parallel thick atmosphere, *Appl. Opt.*, *9*, 1457–1466, 1970.

Delany, A. C., P. Haagensen, S. Walters, A. F. Wartburg, and P. J. Crutzen, Photochemically produced ozone in the emission from large-scale tropical vegetation fires, *J. Geophys. Res.*, *90*, 2425–2429, 1985.

Einfeld, W., D. Ward, and C. Hardy, Effects of fire behavior on prescribed fire smoke characteristics, in *Global Biomass Burning*, pp. 412–419, MIT Press, Cambridge, Mass., 1991.

Ferrare, R. A., R. S. Fraser, and Y. J. Kaufman, Satellite remote sensing of large-scale air pollution—Application to a forest fire, *J. Geophys. Res.*, *95*, 9911–9925, 1990.

Fishman, J., Probing planetary pollution from space, *Environ. Sci. Technol.*, *25*, 512–621, 1991.

Fishman, J., and J. C. Larsen, The distribution of total ozone and stratospheric ozone in the tropics: Implications for the distribution of tropospheric ozone, *J. Geophys. Res.*, *92*, 6627–6634, 1987.

Fishman, J., V. Ramanathan, P. J. Crutzen, and S. C. Liu, Tropospheric ozone and climate, *Nature*, *282*(5741), 818–820, 1979.

Fishman, J., O. P. Minnis, and H. G. Reichle, Jr., Use of satellite data to study ozone in the tropics, *J. Geophys. Res.*, *91*, 14,451–14,465, 1986.

Fraser, R. S., Y. J. Kaufman, and R. L. Mahoney, Satellite measurements of aerosol mass and transport, *J. Atmos. Environ.*, *18*, 2577–2584, 1984.

Greenberg, J. P., P. R. Zimmerman, L. Heidt, and W. Pollock, Hydrocarbon and carbon monoxide emissions from biomass burning in Brazil, *J. Geophys. Res.*, *89*, 1350–1354, 1984.

Hänel, G., An attempt to interpret the humidity dependencies of aerosol extinction and scattering coefficients, *Atmos. Environ.*, *15*, 403–406, 1981.

Hao, W. M., M.-H. Liu, and P. Crutzen, Estimates of annual and regional releases of CO_2 and other trace gases to the atmosphere from fires in the tropics, based on the FAO statistics for the period 1975–1980, in *Fire in the Tropical Biota*, edited by J. G. Goldammer, pp. 440–462, Springer-Verlag, New York, 1990.

Hegg, D. A., L. F. Radke, P. V. Hobbs, R. A. Rasmussen, and P. J. Riggan, Emissions of some trace gases from biomass fires, *J. Geophys. Res.*, *95*, 5669–6675, 1990.

Hobbs, P. V., and L. F. Radke, Cloud condensation nuclei from a simulated forest fire, *Science*, *163*, 279–280, 1969.

Holben, B. N., Y. J. Kaufman, A. Setzer, D. Tanre, and D. E. Ward, Optical properties of aerosol from biomass burning in the tropics, BASE-A, in *Global Biomass Burning*, pp. 403–411, MIT Press, Cambridge, Mass., 1991.

Huntzicker, J. J., and R. L. Johnson, Investigation of an ambient interference in the measurements of ozone by ultraviolet absorption photometry, *Environ. Sci. Technol.*, *13*, 1414–1416, 1979.

(INEMET), (in Portuguese), *Bol. Agroclimatol. Decendial*, nos. 24 and 25, 1989.

Instituto de Pesquisas Espaciais (INPE), *Climanalise* (in Portuguese), vol. 4, nos. 8 and 9, 1989.

Johnson, R., and C. Huntzicker, An automated thermal optical method for the analysis of carbonaceous aerosols, in *Atmospheric aerosol sources—Air quality relationships*, American Chemical Society, Washington, D. C., 1981.

Kaufman, Y. J., Satellite sensing of aerosol absorption, *J. Geophys. Res.*, *92*, 4307–4317, 1987.

Kaufman, Y. J., and M.-D. Chou, Model simulations of the competing climatic effects of SO_2 and CO_2, *J. Clim.*, in press, 1991.

Kaufman, Y. J., and R. S. Fraser, Light extinction by aerosols during summer air pollution, *J. Appl. Meteorol.*, *22*, 1694–1706, 1983.

Kaufman, Y. J., C. J. Tucker, and I. Fung, Remote sensing of biomass burning in the tropics, *J. Geophys. Res.*, *95*, 9927–9939, 1990*a*.

Kaufman, Y. J., R. S. Fraser, and R. A. Ferrare, Satellite remote sensing of large-scale air pollution—Method, *J. Geophys. Res.*, *95*, 9895–9909, 1990*b*.

King, M. D., D. M. Byrne, B. M. Herman, and J. A. Reagan, Aerosol size distribution obtained by inversion of optical depth measurements, *J. Atmos. Sci.*, *35*, 2153–2167, 1978.

Kirchhoff, V. W. J. H., Surface ozone measurements in Amazonia, *J. Geophys. Res.*, *93*(D2), 1406–1476, 1988.

Kirchhoff, V. W. J. H., E. V. Browell, and G. L. Gregory, Ozone measurements in the troposphere of an Amazonian rain forest environment, *J. Geophys. Res.*, *93*(D12), 15,850–15,860, 1988.

Kirchhoff, V. W. J. H., E. V. A. Marinho, P. L. S. D. Dias, R. Calheiros, R. Andre, and C. Volpe, O_3 and CO from burning sugar cane, *Nature*, *339*(6222), 264, 1989*a*.

Kirchhoff, V. W. J. H., A. W. Setzer, and M. C. P. Pereira, Biomass burning in Amazonia: Seasonal effect on atmospheric O_3 and CO, *Geophys. Res. Lett.*, *16*(5), 459–472, 1989*b*.

Lee, T. F., and P. M. Tag, Improved detection of hotspots using the AVHRR 3.7 μm channel, *Bull. Am. Meteorol. Soc.*, *71*(12), 1722–1730, 1990.

Malingreau, J., and C. J. Tucker, Large scale deforestation in the southeastern Amazon basin of Brazil, *Ambio*, *17*, 49–55, 1988.

Matson, M., and J. Dozier, Identification of subresolution high temperature sources using a thermal IR sensor, *Photogramm. Eng. Remote Sens.*, *47*, 1312–1318, 1981.

Matson, M., S. R. Schneider, B. Aldridge, and B. Satchwell, Fire detection using the NOAA-series satellites, *NOAA Tech. Rep. NESDIS-7*, U.S. Dep., Natl. Ocean. Atmos. Admin., Natl. Environ. Satell. Data and Inf. Serv., Natl. Weather Serv., Washington, D. C., 1984.

Menzel, W. P., E. C. Cutrim, and E. M. Prins, Geostationary satellite estimation of biomass burning in Amazonia during BASE-A, *Global Biomass Burning*, MIT Press, Cambridge, Mass., 1990.

Nelson, R. M., Jr., An evaluation of the carbon mass balance technique for estimating emission factors and fuel consumption in forest fires, *Res. Pap. SE-231*, U.S. Dep. of Agric., For. Serv., Southeastern For. Exper. Stn., Asheville, N. C., 1982.

Pereira, M. C. P., Detection, monitoring and analysis of some environmental impacts of biomass burning in Amazonia through NOAA and Landsat satellites and aircraft data (in Portuguese), M.Sc. dissertation, *INPE-4503-TDL/326*, 268 pp., Inst. de Pesqui. Espaciais, 1988.

Prins, E. M., and W. P. Menzel, Geostationary satellite detection of biomass burning in South America, *Int. J. Remote Sens.*, in press, 1990.

Pueschel, R. F., J. M. Livingston, P. B. Russell, D. A. Colburn, T. P. Ackerman, D. A. Allen, B. D. Zak, and W. Einfeld, Smoke optical depths: Magnitude, variability, and wavelength dependence, *J. Geophys. Res.*, *93*, 8388–8402, 1988.

Radke, L. F., Airborne observations of cloud microphysics modified by anthropogenic forcing, in *Symposium on Atmospheric Chemistry and Global Climate, Jan. 29–Feb. 3, Anaheim, Calif.*, pp. 310–315, American Meteorological Society, Boston, Mass., 1989.

Radke, L. F., J. L. Stith, D. A. Hegg, and P. V. Hobbs, Airborne studies of particles and gases from forest fires, *J. Air Pollut. Control. Ass.*, *28*, 30–34, 1978.

Radke, L. F., J. H. Lyons, P. V. Hobbs, D. A. Hegg, D. V. Sandberg, and D. E. Ward, Airborne monitoring and smoke characterization of prescribed fires on forest lands in western Washington and Oregon, *Gen. Tech. Rep. PNW-GTR-251*, U.S. Dep. of Agric., For. Serv., Pacific Northwest Res. Stn., Portland, Oreg., 1990.

Radke, L. F., D. A. Hegg, P. V. Hobbs, J. D. Nance, J. H. Lyons, K. K. Laursen, P. J. Reagan, and D. E. Ward, Particulate and trace gas emission from large biomass fires in North America, in *Global Biomass Burning*, pp. 209–224, MIT Press, Cambridge, Mass., 1991.

Ramanathan, V., R. J. Cicerone, H. B. Singh, and J. T. Kiehl, Trace gas trends and their potential role in climate change, *J. Geophys. Res.*, *90*, 5547–5566, 1985.

Seiler, W., and P. J. Crutzen, Estimates of gross and net fluxes of carbon between the biosphere and the atmosphere from biomass burning, *Clim. Change*, *2*, 207–247, 1980.

Setzer, A. W., and M. C. P. Pereira, Project SEQE report for 1988—Remote sensing of biomass burning (in Portuguese), *INPE Intern. Rep.*, in press, 1990.

Setzer, A. W., and M. C. Pereira, Amazonia biomass burnings in 1987 and an estimate of their tropospheric emissions, *Ambio*, *20*, 19–22, 1991.

Setzer, A. W., M. C. P. Pereira, A. C. P. Pereira, and S. O. Almeida, Relatorio de atividades do projeto IBDF-INPE "SEQE"-ANO 1987, *INPE Publ.*, *INPE-4534-RPE/565*, Inst. de Pesqui. Espaciais, 1988.

Setzer, A. W., V. W. J. H. Kirchhoff, and M. C. P. Pereira, Ozone concentrations in the Brazilian Amazonia during BASE-A, in *Global Biomass Burning*, pp. 112–114, MIT Press, Cambridge, Mass., 1991.

Squires, P., and S. Twomey, The relation between cloud droplet spectra and the spectrum of cloud nuclei, in *Physics of Precipitation, Geophys. Monogr. Ser.*, vol. 5, pp. 211–219, 1960.

Stith, J. L., L. F. Radke, and P. V. Hobbs, Particle emission and the production of ozone and nitrogen oxides from the burning of forest slash, *Atmos. Environ.*, *15*, 73–82, 1981.

Tanré, D., C. Devaux, M. Herman, R. Santer, and Y. J. Gao, Radiative properties of desert aerosols by optical ground measurements at solar wavelengths, *J. Geophys. Res.*, *93*, 14,223–14,231, 1988.

Tucker, C. J., B. N. Holben, and T. E. Goff, Intensive forest clearing in Rondonia, Brazil, as detected by satellite remote sensing, *Remote Sens. Environ.*, *15*, 255, 1984.

Twomey, S. A., The influence of pollution on the short wave albedo of clouds, *J. Atmos. Sci.*, *34*, 1149–1152, 1977.

Twomey, S. A., and J. Warner, Comparison of measurements of cloud droplets and cloud nuclei, *J. Atmos. Sci.*, *24*, 702–703, 1967.

Twomey, S. A., M. Piepgrass, and T. L. Wolfe, An assessment of the impact of pollution on the global albedo, *Tellus*, *36*(b), 356–366, 1984.

Ward, D. E., Field scale measurements of emission from open fires, technical paper presented at the Defense Nuclear Agency Global Effects Review, Def. Nucl. Agency, Washington, D. C., 1986.

Ward, D. E., and C. C. Hardy, Advances in the characterization and control of emissions from prescribed fires, *Proc. Annu. Meet. APCA*, 1984.

Ward, D. E., and C. C. Hardy, Smoke emissions from wildland fires, *Environ. Int.*, *17*, 1991.

Ward, D. E., C. C. Hardy, R. D. Ottmar, and D. V. Sandberg, A sampling system for measuring emissions from west coast prescribed fires, paper presented at the Pacific Northwest International Section of the Air Pollution Control Association, 10 pp., Vancouver, B. C., Canada, 1982.

Ward, D. E., C. C. Hardy, D. V. Sandberg, and T. E. Reinhardt, III, Emissions characterization, in Mitigation of Prescribed Fire Atmospheric Pollution Through Increased Utilization of Hardwoods, Piled Residues, and Long-Needled Conifers, compiled by D. V. Sandberg, D. E. Ward, R. D. Ottmar, et al., final report to the Bonneville Power and U.S. Dep. of Energ. under IAG DE-AI179-85BP18509 (PNW-85-423), July 15, 1989.

Ward, D. E., A. Setzer, Y. Kaufman, and R. Rasmussen, Characteristics of smoke emissions from biomass fires of the Amazon region—BASE-A experiment, in *Global Biomass Burning*, pp. 394–402, MIT Press, Cambridge, Mass., 1991.

Ward, D. E., R. Susott, J. Kauffman, R. Babbitt, B. N. Holben, Y. J. Kaufman, A. Setzer, R. Rasmussen, D. Cummings, and B. Dias, Smoke and fire characteristics for cerrado and deforestation burns in Brazil—BASE-B experiment, *J. Geophys. Res.*, this issue.

Warner, J., and S. A. Twomey, The production of cloud nuclei by cane fires and the effect on cloud droplet concentration, *J. Atmos. Sci.*, *24*, 704–707, 1967.

Whitby, K. T., The physical characteristics of sulfur aerosols, *Atmos. Environ.*, *12*, 135–159, 1978.

Wigley, T. M. L., Possible climate change due to SO_2 derived cloud condensation nuclei, *Nature*, *339*, 355–357, 1989.

Woodwell, G. M., J. E. Hobbie, R. A. Houghton, J. M. Melillo, B. Moore, B. J. Peterson, and G. R. Shaver, Global deforestation: Contribution to atmospheric carbon dioxide, *Science*, *222*, 1081–1086, 1983.

B. N. Holben and D. Tanre, NASA Goddard Space Flight Center, Mail Code 923, Greenbelt, MD 20771.

Y. J. Kaufman, NASA Goddard Space Flight Center, Mail Code 913, Greenbelt, MD 20771.

P. Menzel, NOAA/NESDIS Satellite Applied Laboratory, 1225 West Dayton Street, Madison, WI 53706.

M. C. Pereira and A. Setzer, INPE C. Postal 515, 12201, S. J. Campos, São Paulo, Brazil.

R. Rasmusson, Oregon Graduate Institute, Beaverton, OR 97005.

D. Ward, USDA Forest Service Fire Chem., P. O. Box 8089, Missoula, MT 59807.

(Received July 30, 1991;
revised February 3, 1992;
accepted February 3, 1992.)